Petrological and geochemical investigations of potential source rocks of the central Congo Basin, Democratic Republic of Congo

Victoria F. Sachse, Damien Delvaux, and Ralf Littke

ABSTRACT

Paleozoic and Mesozoic outcrop and core samples (REMINA Dekese and REMINA Samba wells) covering various stratigraphic intervals from the central Congo Basin were analyzed for total organic carbon (C_{org}), total inorganic carbon (C_{inorg}), and total sulfur content. Rock-Eval analysis and vitrinite reflectance (R_o) measurements were performed on the basis of the C_{org} content. Fifteen samples were chosen for molecular organic geochemistry. Nonaromatic hydrocarbons (HCs) were analyzed by gas chromatography (GC)–flame ionization detection and GC–mass spectrometry.

Samples of the Alolo shales from the Aruwimi Group (Lindi Supergroup, late Neoproterozoic to early Paleozoic) are in general very poor in C_{org} (most samples <0.5%) and contain a high amount of degraded organic matter (OM). All samples of this group revealed a type III to IV kerogen and cannot be considered as a potential source rock. Permian–Carboniferous sediments from the Lukuga Group (Dekese well and outcrop samples) contain moderate contents of organic carbon (<2%). The T_{max} values (heating temperature at which the top peak of S_2 occurs) indicate early mature OM, partly also a higher level of maturity because of R_o (0.6–0.7%) and production index values ($S_1/S_1 + S_2 < 0.2$). All samples contain hydrogen-poor type III to IV kerogen with low HC generation potential, only having a very minor gas generation potential. The kinds of OM, as well as the biological markers, indicate a terrestrial-dominated depositional environment.

Manuscript received February 22, 2011; provisional acceptance May 5, 2011; revised manuscript received May 19, 2011; final acceptance July 12, 2011.
DOI:10.1306/07121111028

AUTHORS

VICTORIA F. SACHSE ~ *Institute for Geology and Geochemistry of Petroleum and Coal, Lochnerstrasse 4-20, RWTH (Rheinisch-Westfaelische Technische Hochschule) Aachen University, 52056 Aachen, Germany; sachse@lek.rwth-aachen.de*

Victoria Sachse received her degree in geology at RWTH (Rheinisch-Westfaelische Technische Hochschule) Aachen University in 2008 and has just finished her Ph.D. thesis at the Institute of Geology and Geochemistry of Petroleum and Coal, RWTH Aachen University. Her research interests are related to petroleum systems modeling and petroleum source rock studies with a main regional focus on West Africa.

DAMIEN DELVAUX ~ *Royal Museum for Central Africa, B-3080 Tervuren, Belgium; damien.delvaux@africamuseum.be*

Damien Delvaux is a senior structural geologist working at the Royal Museum for Central Africa (RMCA) since 1989 on continental rift systems, tectonic control of sedimentary basin evolution, and tectonic stress. The RMCA is hosting unique reference archives and geologic sample collections from outcrop and borehole for the entire Democratic Republic of Congo on the basis of which this work has been done.

RALF LITTKE ~ *Institute for Geology and Geochemistry of Petroleum and Coal, Lochnerstrasse 4-20, RWTH (Rheinisch-Westfaelische Technische Hochschule) Aachen University, 52056 Aachen, Germany; littke@lek.rwth-aachen.de*

Ralf Littke is a professor of geology and geochemistry of petroleum and coal at RWTH (Rheinisch-Westfaelische Technische Hochschule) Aachen University. His primary research interest is sedimentary basin dynamics. Littke has been a member of AAPG since 1986.

ACKNOWLEDGEMENTS

We thank U. Glasmacher, University of Heidelberg, for fruitful discussions of thermal maturity and unpublished fission-track data. D. Delvaux was supported by the Belgian Federal Science Policy, Action 1 program. We gratefully acknowledge thoughtful reviews by J. A. Bojesen-Koefoed, I. Davison, and S.G. Henry on a previous version of this manuscript. Chris Cornford is

gratefully acknowledged for provision of pIGI (Integrated Geochemical Interpretation [IGI] Ltd.). The AAPG Editor thanks the following reviewers for their work on this paper: Jorgen A. Bojesen-Koefoed, Ian Davison, and Steven G. Henry.

Organic geochemical investigations on Upper Jurassic (Stanleyville Group) to Lower Cretaceous (Loia Group) samples from the Samba well and outcrops in the northeastern part of the Congo Basin reveal moderate to high contents of organic carbon (as much as 25%). The kerogen has very high hydrogen index (HI) values reflecting type I kerogen of excellent quality in the Stanleyville Group (as much as 900 mg HC/g C_{org}) and type I to II kerogen in the overlying Loia Group (as much as 900 mg HC/g C_{org}). Outcrop samples from the Stanleyville Group have variable partly high C_{org} contents and are also characterized by very high HI values (as much as 900 mg HC/g C_{org}). The samples studied are too immature for petroleum generation. Based on biomarker analysis, an aquatic anoxic depositional environment can be assumed for the Stanleyville Group, whereas a lacustrine deposition is likely for the samples of the Loia Group. Based on the geologic knowledge of the area, deposition under lacustrine conditions is most likely also for the Stanleyville Group. Both the Stanleyville and Loia groups can be regarded as excellent petroleum source rocks and could be part of a petroleum system if sufficient burial and maturation have occurred. The presence of resedimented vitrinite particles in the Lukuga Group of the Dekese well with a slightly higher maturation rank than the autochthonous vitrinites suggests that 3000–4000 m (9840–13,120 ft) of Carboniferous to Devonian sediment has been eroded from the eastern margin of the Congo Basin.

Finally, R_o data were used to create one-dimensional models for the Dekese and Samba wells, giving an overview of the burial, thermal, and maturity histories of the area.

INTRODUCTION

Intracontinental sedimentary basins contain some of the world's major hydrocarbon (HC) provinces, for example, the giant gas resources of West Siberia (Surkov et al., 1991; Kontorovich et al., 1996; Littke et al., 2008). Some of the source rocks in rift-related continental basins were deposited under lacustrine conditions (e.g., Upper to Lower Cretaceous of Africa and South America; also Songliao Basin, northern China; Paleozoic of western China and Tertiary of eastern China and Southeast Asia; Harris et al., 2004). In later rifting stages, potential source rocks were also deposited under deltaic and marine conditions. Katz (1995) assumed that source rock accumulations are richest during the active rift stage, when rift-related lakes reach their greatest depth and extension. Commonly, anoxic bottom-water conditions prevailed during this phase of rift lake development.

One exception is the Sudan rift basin, where the source rocks are related to the deposition of lacustrine sediments under shallow-water conditions during late rift phase (Schull, 1988), and a significant increase in the organic matter (OM) content occurred from the early to late rift stage. In general, three critical factors have been identified for the deposition of organic-rich sediments: (1) high bioproductivity, including high nutrient flux (Pedersen and Calvert, 1990); (2) slow sediment accumulation that does not dilute the OM (Tyson, 2001); and (3) oxygen-depleted (anoxic) conditions that limit oxidation reactions in the water column and in the shallow sediments (Demaison and Moore, 1980).

The Congo Basin is one of the largest intracratonic sedimentary rift basins in the world (covers a total of 3.7 million km^2 [1.4 million mi^2]) but still poorly investigated with respect to petroleum potential. Between 1950 and 1980, geophysical investigations and data from four wells (Esso Zaire Mbandaka, Esso Zaire Gilson, REMINA Samba, and REMINA Dekese) gave further insight into the structure of the Congo Basin and the deposited sequences. Results of the first exploration campaign (gravimetry, refraction seismics, field mapping, and drilling of the Samba and Dekese stratigraphic boreholes) by REMINA (1952–1956) are synthesized in Cahen et al. (1959, 1960) and Evrard (1957, 1960), whereas the second exploration phase was conducted by Shell, Texaco, and Japan National Oil Corporation (JNOC) (1970–1984; seismic reflection, field investigations, and drilling of the Mbandaka, Gilson exploration boreholes). Only short syntheses have been published by Lawrence and Makazu (1988) and by Daly et al. (1992). Limited geochemical and petrological characterization of samples from potential source rock units was undertaken several years after the REMINA campaign on samples from outcrops and boreholes stored at the Royal Museum for Central Africa. A more systematic geochemical and petrological investigation of source rocks was based on new outcrop samples collected during the JNOC 1984 campaign, focusing on the Lower Cretaceous sandstones of the Kananga region and the Jurassic bituminous shales of the Kisangani region. The source rocks of the more than 4000 m (>13,120 ft) deep Gilson and Mbandaka wells have been analyzed in detail, but the results are not publicly available and all the sample material has been lost. As a result, the present knowledge on the source rock characteristics remains incomplete and mostly confidential. This fact presents an important limiting factor for the understanding of the HC system of this huge basin. Up to now, the investigations by Daly et al. (1991, 1992) contain the most comprehensive source information on the intracratonic Congo Basin, including the basin structure and its post-Paleozoic history. In addition, Giresse (2005) compiled the Mesozoic–Cenozoic history of the intracratonic Congo Basin, and Kadima et al. (2011a, b) proposed a revision of the stratigraphic and tectonic evolution of the Congo Basin since the late Neoproterozoic. This article documents various types of source rocks in the Congo Basin; the quantity, quality, and maturity of OM; and the depositional environment in relation to tectonic evolution. For this purpose, a total of 147 samples stored in the rock collection of the Royal Museum for Central Africa, Belgium, covering various stratigraphic units of the intracratonic Congo Basin, were investigated, including two wells (Samba and Dekese; Figures 1, 2).

GEOLOGIC SETTING

Overview

The Congo Basin is a broad and long-lived intracratonic depression in the center of the African plate covering most of the Democratic Republic of Congo (DRC, formerly Zaire), the People's Republic of Congo, and the Central African Republic, coinciding with a region of pronounced long-wavelength gravity anomaly (Crosby et al., 2010) (Figure 1). It has a long history of sediment accumulation, tectonic inversion, and erosion since the Neoproterozoic (Veatch, 1935; Cahen and Lepersonne, 1954; Lepersonne, 1977; Daly et al., 1992; Giresse, 2005; Kadima et al., 2011a) and is still tectonically active (Delvaux and Barth, 2010). According to Daly et al. (1992) and Kadima et al. (2011a, b), the evolution of the Congo Basin started

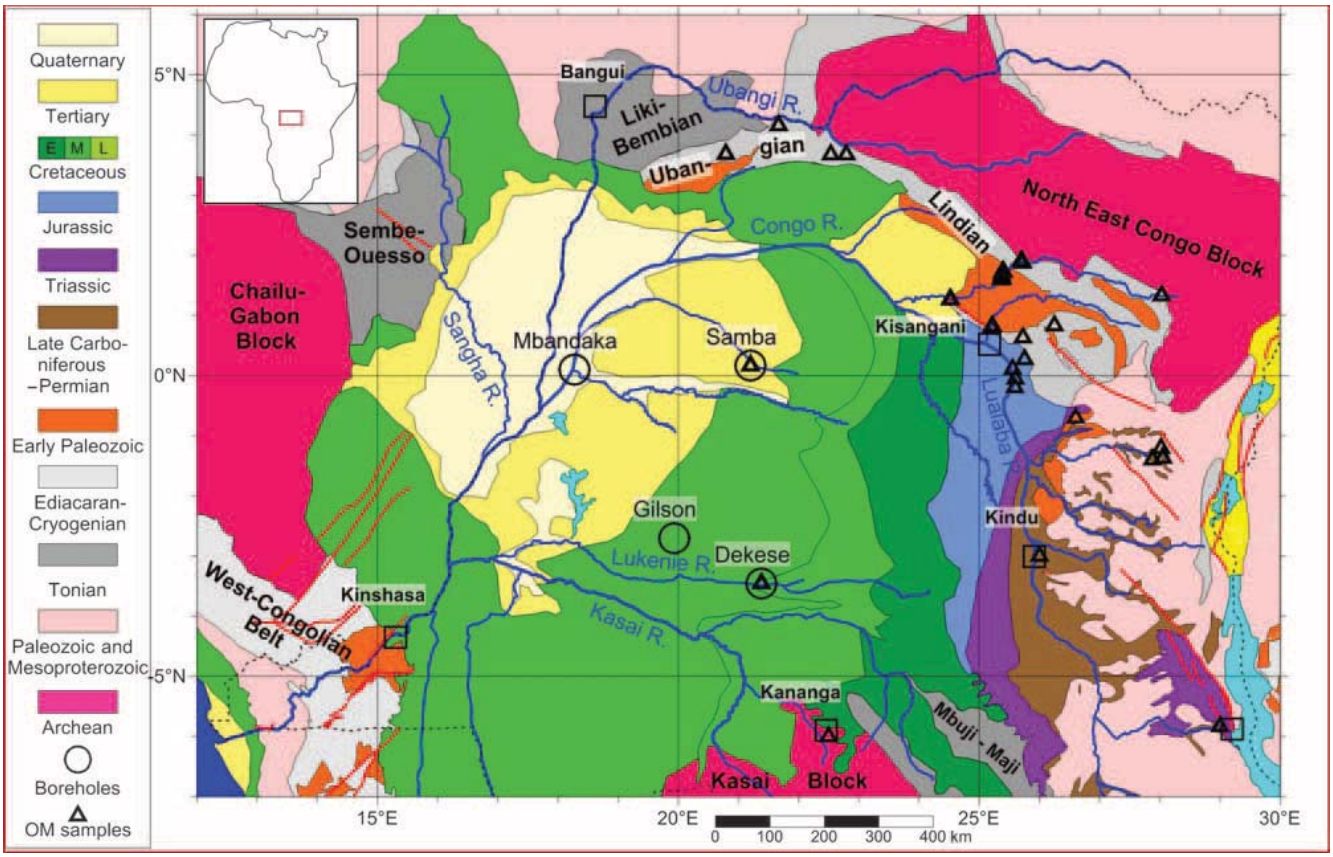

Figure 1. Simplified map of the Congo Basin with location of the sample sites. OM = organic matter.

in the Neoproterozoic probably in an intracratonic extensional context. The subsequent subsidence is at least partly related to the cooling of the stretched lithosphere during the Paleozoic and was affected by several basin inversion periods. The late Cenozoic subsidence is possibly controlled by the action of a downward dynamic force on the lithosphere either related to a high-density object at the base of the lithosphere (Downey and Gurnis, 2009; Crosby et al., 2010) or in response to a downwelling mantle plume (Forte et al., 2010) or to delamination (Buitler and Steiberger, 2010).

The stratigraphic evolution of the Congo Basin is incompletely known because of its large dimensions and limited exposure and exploration work. The general stratigraphic evolution has been synthesized by Lawrence and Makazu (1988) and Daly et al. (1992) based on the results of two exploration campaigns, correlating well stratigraphy with field-based observations. A synthetic stratigraphic column was presented by Daly et al. (1992), assuming long-distance lateral continuity of the groups. However, this concept appears to be of limited applicability as the stratigraphic units vary laterally both in facies and thickness, some of them being of limited extent and locally missing. A revised and more detailed stratigraphy is presented in Kadima et al. (2011a, b), considering the spatial distribution of the observations (Figure 2).

Summary of the Tectonostratigraphic Evolution

The development of the Congo Basin appears to be controlled by a series of events, defining three first-order sedimentary units that are separated by prominent seismic reflectors and broadly correlated to the Neoproterozoic, Paleozoic, and Mesozoic–Cenozoic.

Sedimentation started in the Neoproterozoic during a poorly defined intracratonic rifting stage that failed to develop into a real continent breakup. The postrift subsidence controlled the deposition of a first sedimentary unit during the Cryogenian and the Ediacaran. This sequence is known

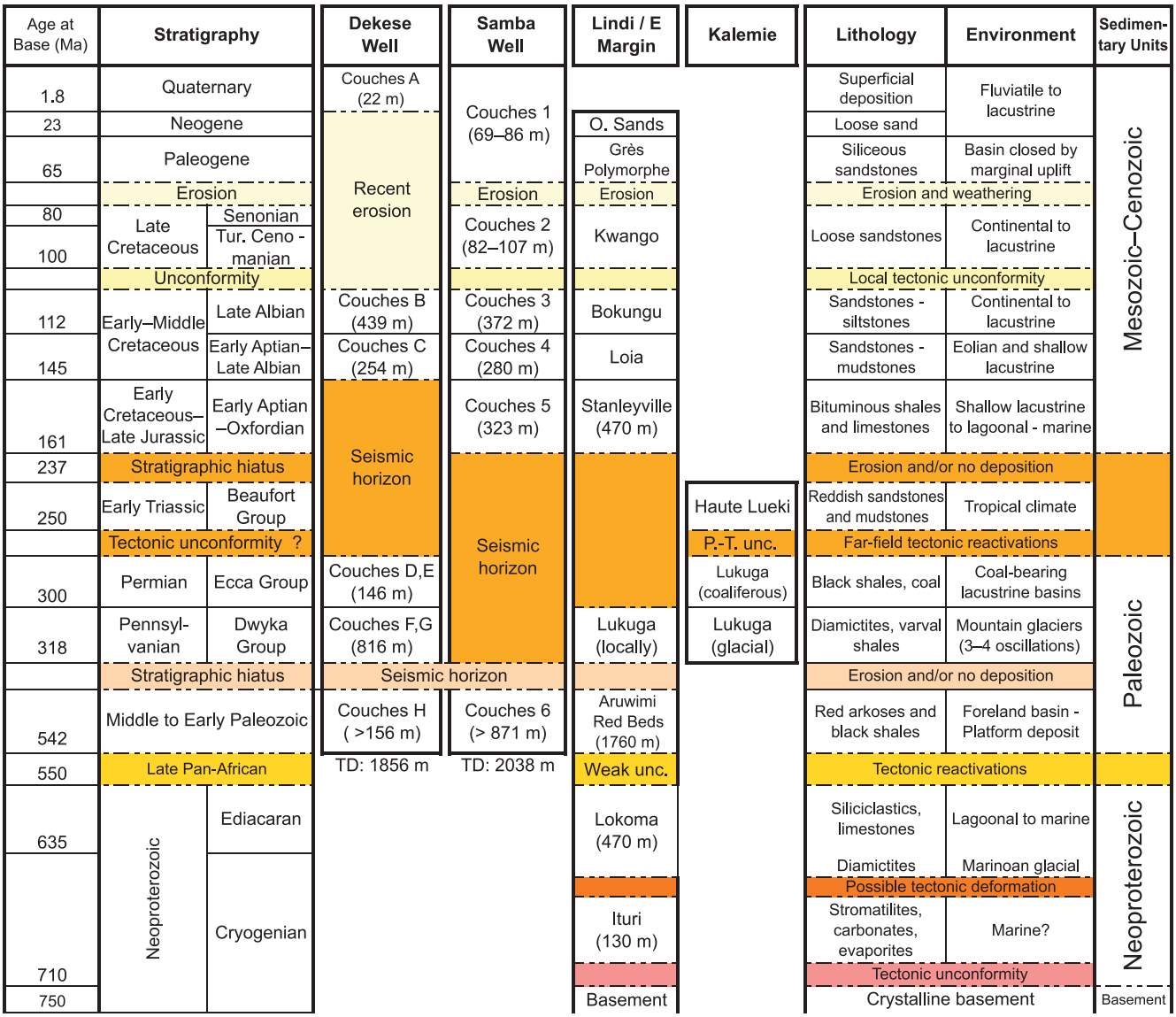

Figure 2. Overview on stratigraphic units within the Congo Basin (modified from Kadima et al., 2011b). Note that the term "couches" refers to the English term "beds."

from the work of Verbeek (1970) in the Lindi-Aruwimi region, north of Kisangani. In this type region, it is composed of approximately 130 m (~430 ft) of stromatolitic carbonates at the base (Ituri Group), followed by approximately 470 m (~1540 ft) of siliciclastics and limestone (Lokoma Group) deposited in an environment interpreted as lagoonal to marine. These units are further subdivided into Penge arkoses (10–20 m [33–66 ft]), Lenda carbonates with carbonaceous layers (80–130 m [262–430 ft]), and Asoso shales and sandstones (50 m [164 ft]) for the Ituri Group and Akwokwo tillites (0–40 m [33–130 ft]), Bobwamboli conglomerates and arkoses (50–250 m [164–820 ft]), Mamungi gray shales and limestones (200–500 m [656–1640 ft]) and Kole shales (100 m [328 ft]) for the Lokoma Group (Figure 2).

Above a marked unconformity in the seismic profiles, which is, however, weakly expressed in the Lindi-Aruwimi region, a thick (1760 m [5774 ft]) sequence of Paleozoic siliciclastics follows, which is dominated by red arkoses, and forms the Aruwimi Group. Verbeek (1970) subdivided this unit successively into Galamboge quartzites with cross-bedding (100–150 m [328–492 ft]), Alolo carbonaceous dark shales (350–400 m [1148–1312 ft]), and Banalia red arkoses with cross-bedding (as much as 1200 m [3937 ft]), with transitional approximately 100-m

(~328-ft)-thick transitional units between them. The Alolo shales were probably deposited in a shallow-marine to lagoonal basin. The Banalia red arkoses are overlain by glacial-interglacial and postglacial sediments of the Lukuga Group (816 and 146 m [2677 and 479 ft], respectively, in the Dekese well), attributed to the Pennsylvanian–Permian. This age for the Aruwimi Group is problematic and constrained only by the Pan-African unconformity (~550–542 Ma) at the base and by the Pennsylvanian–Permian sediments of the Lukuga Group on top, spanning the entire early–middle Paleozoic. No prominent discontinuities can be seen between the Aruwimi and the Lukuga groups either in the Dekese core or in the seismic profiles. In consequence, they have been grouped into a single sedimentary unit representing the known Paleozoic in the Congo Basin. The stratigraphy of the Lukuga Group contains a series of glacial to periglacial massive diamictites and varval dark-gray shales deposited under water in a large basin in front of mountain glaciers in the Dekese area (couches F–G) or as morainic deposits in the region of Kalemie during several glacial oscillations. They are overlain by postglacial black shales in the Dekese area (couches D–E) or sandstones with coal seams in the Kalemie region along the western shore of Lake Tanganyika (Lukuga coal field) (Fourmarier, 1914; Jamotte, 1931; Cahen et al., 1959).

A marked discontinuity separates the Paleozoic sedimentary unit from the overlying Mesozoic–Cenozoic series assembled into a third sedimentary unit. The Mesozoic sedimentation began in the eastern rim of the Congo Basin with Triassic reddish sandstones and mudstones in the Kalemie region (Haute Lueki Group), overlying unconformably the Permian sediments in the Lukuga coal field. At Kisangani (former Stanleyville) and south of it along the upper course of the Congo River (also named Lualaba), 470 m (1542 ft) of sandstones with bituminous shales and limestones of the Late Jurassic to Early Cretaceous (Oxfordian–early Aptian) represent lacustrine deposits, assembled into the Stanleyville Group (Passau, 1923; Lombard, 1960; Lepersonne, 1977, Cahen, 1983a; Colin, 1994). Toward the basin center in the Samba well, 323 m (1060 ft) of fluvial-lacustrine red sandstones with thin layers of bituminous shales are attributed to the Stanleyville Group, directly overlying the Aruwimi Group (couches 5; Cahen et al., 1959). The Stanleyville Group is absent in the Dekese well (Cahen et al., 1960) and occurs in a condensed section in the Kinshasa area (Egorov and Lombard, 1962). The depositional area of the overlying Loia Group (upper Aptian–lower Albian) enlarged considerably, and its depocenter shifted toward the present center of the basin, whereas the southern and eastern rims of the basin were uplifted (Lepersonne, 1977; Cahen, 1983b). The Loia Group is represented in the Dekese well by 254 m (833 ft) of eolian sand dunes (couches C) and in the Samba well by 280 m (918 ft) of shallow lacustrine sandstones and mudstones with bituminous shale levels (Cahen et al., 1959, 1960; Linol et al., 2011).

The stratigraphic succession continues with the upper Albian Bokungu fluviodelatic sandstones and siltstones (372–439 m [1220–1440 ft] in the wells), unconformably overlain by the Late Cretaceous Kwango Group. The Kwango Group has been defined and dated paleontologically in the Kwango River region on the southwestern side of the DRC, where the complete section contains the Turonian to Late Cenomanian Inzia formation and the Maastrichtian–Senonian N'Sele Formation (Lepersonne, 1951, 1977; Colin, 1994). A slight unconformity with a basal conglomerate exists between the Kwango and the Bokungu groups. The Kwango Group is not represented in the Dekese well because of recent river incision erosion (the Dekese well is located in the floor of a valley where the Kwango Formation is outcropping on the flanks). In the Samba well, the 280-m (918-ft)-thick couches C, composed of pure quartz sand and kaolin-bearing clay, are correlated to the Kwango Formation but do not contain datable material (Cahen et al., 1959). They are, however, markedly different mineralogically from the underlying Bokungu feldpathic sandstones that do not contain kaolin. A recent reexamination of the contact between these two formations shows that it is fault controlled (Kadima et al., 2011).

The Paleogene is represented by the Grès Polymorphe Group, composed of silicified eolian sands deposited over a prominent erosion surface, and

surmounted by the Neogene Ochre Sands (70–90 m [230–295 ft] in total for the Cenozoic) (Cahen et al., 1959, 1960, 1983b; Lepersonne, 1977; Linol et al., 2011).

This review shows that the sedimentary units and discontinuities at the scale of the basin present strong lateral variations in thickness and facies. In particular, the Paleozoic–Mesozoic discontinuity spans the entire Triassic and Jurassic in the Samba well, the Permian and Triassic in the Dekese well, and is almost absent in the Kalemie area. This loosely constrained period would correspond to an important compressional basin inversion (Daly et al., 1992) that has been related to far-field effects during the Late Permian–Early Triassic development of the Cape fold belt of South Africa (Hälbich et al., 1983; Le Roux, 1995; Delvaux, 2001; Newton et al., 2006; Tankard et al., 2009).

SAMPLES AND METHODS

A total of 147 samples were made available from the Royal Museum of Central Africa, Tervuren, Belgium. They include outcrop samples of the Neoproterozoic (Lenda limestones, Ituri Group, and Mamungi shales, Lokoma Group) in the Lindi and Ubangui regions, middle–lower Paleozoic (Alolo shales, Aruwimi Group) north of Kisangani, Pennsylvanian–Lower Permian (lower glacial to periglacial part of Lukuga Group) in the Walikale area (North Kivu), Upper Jurassic–Lower Cretaceous (Stanleyville Group) along the upper Congo River (Lualaba), in Kisangani and south of it (Figures 1, 2). In addition, samples from the Dekese and Samba wells were collected from the Loia, Stanleyville, and Lukuga groups. One coal sample of mid-Permian postglacial age from the Lukuga coal field near Kalemie along the congolese shore of Lake Tanganyika was also investigated (Figure 1). Only organic-rich levels of these groups have been sampled instead of a systematic sampling, and the results obtained in this work do not represent the quantitative average composition of the sampled units but instead have been used to qualify the OM type and maturation in terms of source rock potential and depositional environment. Samples from the Lindian Supergroup have been collected by Verbeek (1970), with most of the Alolo shale samples close to a fault zone.

Total inorganic carbon (C_{inorg}) and total organic carbon (C_{org}) were measured with a Leco RC-412 carbon analyzer via infrared absorption. Total carbon (C_{total}) concentrations were determined using $C_{total} = C_{inorg} + C_{org}$. The $CaCO_3$ percentages were calculated using $CaCO_3 = 8.333\ C_{inorg}$. Total sulfur (TS) concentrations were measured using a Leco S-200 sulfur analyzer with a precision of less than 5% error and a detection limit of 0.0001%. Rock-Eval pyrolysis was performed on 60 samples having C_{org} contents more than 0.4%. Approximately 100 mg of powdered rock was heated in the helium stream of a Delsi, Inc., Rock-Eval II instrument. A detailed description of the procedure is given in Espitalié et al. (1985). Parameters determined by Rock-Eval pyrolysis include hydrogen index (HI = mg HC equivalents/g C_{org}), oxygen index (OI = mg CO_2/g C_{org}), and T_{max} (temperature of maximum pyrolysis yield). A modified Van Krevelen diagram (HI vs. OI) and a crossplot of S_2 and C_{org} were used for kerogen classification. Vitrinite reflectance (R_o) was measured on samples with C_{org} more than 0.4%. For microscopic studies, samples were embedded in an epoxy resin, and a section perpendicular to bedding was polished (Taylor et al., 1998). The polished blocks were investigated at a magnification of 500× in incident white light and in incident light fluorescence mode, excited by ultraviolet and violet light. The R_o measurements were conducted using a Zeiss Axioplan incident light microscope at a wavelength (λ) of 546 nm with a Zeiss Epiplan-Neofluar 50×, 0.85 oil objective. An yttrium aluminum garnet standard was used, with an R_o of 0.889%. For samples rich in vitrinite or solid bitumen particles, at least 50 measurements were made. Mean R_o and standard deviation values were calculated using the Diskus Fossil software (Carl H. Hilgers Technisches Büro). In total, 43 samples were studied by way of reflected light microscopy.

Fifteen samples were selected for molecular organic geochemistry based on their C_{org} and Rock-Eval data. The analysis of nonaromatic HCs was

conducted on 10-g aliquots of each sample extracted with dichloromethane (DCM; 40 mL) and hexane (40 mL) using ultrasonic treatment. The extracts were fractionated by polarity chromatography into nonaromatic HCs (5 mL pentane), aromatic HCs (5 mL pentane and DCM at a ratio of 4:6), and heterocompounds (5 mL MeOH). Gas chromatography (GC) of nonaromatic HCs was performed on a Fisons Instruments GC 8000 series ECD 850 equipped with an on-column injector, a Zebron ZB-1 HT Inferno fused silica capillary column (30-m × 0.25-mm inner diameter; film thickness, 0.25 μm) and a flame ionization detector. Hydrogen was used as the carrier gas. The oven temperature was programmed from 80°C (3 min) to 300°C (held 20 min) at 10°C/min.

The biomarkers were determined by GC–mass spectrometry (GC-MS) using a Finnigan MAT 95SQ mass spectrometer coupled to a Hewlett Packard Series II 5890 gas chromatograph. The spectrometer was operated in electron ionization mode at an ionization energy of 70 eV and a source temperature of 260°C. The chromatograph was equipped with a splitless injector and a Zebron ZB-1 fused silica capillary column (30 m × 0.25 mm; film thickness, 0.25 μm). Helium was used as carrier gas. The oven temperature was programmed from 80 to 310°C (held 3 min) at 5°C/min.

NUMERICAL BASIN SIMULATION

The thermal and depositional evolution of sedimentary basins can be reconstructed by computer-aided models. For obtaining a reliable model, compiling and quantification of geologic, physical, and chemical processes that have occurred during basin development are necessary. Calibration data based on investigations of sediment samples representative of the investigated site are a fundamental input for a basin simulation to generate scenarios as close as possible to reality. Principles of basin modeling were described by Welte and Yalcin (1987) and principles of one-dimensional (1-D) model calibration by Senglaub et al. (2006). The major outcomes of basin modeling approaches are burial, temperature, and maturation histories. The basin evolution is separated into chronological events with a defined age. Each event represents a time of sedimentation, erosion, or nondeposition (Wygrala, 1988). The temperature history is dependent on the heat input into the system, the heat transfer (conduction and convection), and the heat distribution. The temperature history results from the burial history, the petrophysical properties of the rocks, as well as spatial- and time-specific (paleo-) heat-flow data. For optimization of the model, calibration procedures are required. The R_o is the most important calibration parameter. By leveling the input parameters, evolution scenarios can be modified until the modeled calibration parameters match the values measured during the investigation of the sediment samples considered representative for the sequences in the modeled basin. Frequently leveled input parameters during model calibration are, for example, erosion thickness and heat flow (Petmecky et al., 1999; Senglaub et al., 2006). For calculation of the R_o by means of the software PetroMod (Schlumberger IES, version 10), the Easy $\%R_o$ algorithm of Sweeney and Burnham (1990) has been chosen. It is applicable for the R_o range between 0.3 and 4.6%.

Based on the recent geologic setting of the Congo Basin, known geologic processes through time, heat-flow estimation (i.e., Daly et al., 1992; Sebagenzi et al., 1993; Giresse, 2005), and R_o as calibration data, 1-D models of the Dekese and Samba wells were created.

RESULTS

Elemental Analysis

The highest C_{org} values were found for well and outcrop samples of the Loia and Stanleyville groups, with values as much as 25% for samples of the Stanleyville Group (Table 1; Figure 3A). For the samples of the Lukuga Group, low to moderate (<2%) C_{org} values were measured (Table 1). An exception is the coal that has a C_{org} content of 48% and a $CaCO_3$ content of approximately 3% (Figure 3A). Samples of the Aruwimi, Ituri, and Lokoma groups generally have the lowest C_{org}

contents, with mean values less than 0.2%. The C_{inorg} content and, thus, the $CaCO_3$ content are generally low (<35%) for the Lukuga, Loia, Stanleyville, and Lokoma groups. High C_{inorg} and $CaCO_3$ values were recorded only for samples of the Aruwimi and the Ituri groups, with $CaCO_3$ values as much as 99% (Figure 3A). The $CaCO_3$ contents of the Stanleyville Group show an increase in C_{inorg} with a decrease in C_{org} (Figure 3A).

The sulfur content is highly variable, especially in samples of the Aruwimi and Loia groups. The highest values (as much as 4.4%) occur in the Aruwimi and Loia groups. The lowest values were measured for the samples of the Stanleyville and Lukuga groups, which had values less than 0.6%. The Lukuga coal sample also revealed a low TS content (0.5%; Table 1). The Lokoma Group revealed a high amount of TS (2.69%), leading to a very high TS/C_{org} ratio of 14.16 (Figure 3B). In the Lukuga Group, because of high C_{org} values, the respective TS/C_{org} values are only moderate to low, ranging between 0.01 and 0.16. The TS/C_{org} values of the Stanleyville Group are highly variable because of the variable contents of C_{org} (0.05–0.8). High TS/C_{org} values seem to be characteristic of the Aruwimi Group, which has values as much as 4.97 (Figure 3B). Especially in the Aruwimi Group, most of the sulfur is present as pyrite, as demonstrated by microscopic examination.

Rock-Eval Pyrolysis

The Rock-Eval pyrolysis data for samples of the Stanleyville Group revealed a range of the HI from 786 to 1028 mg HC/g C_{org} in the samples of the Lualaba area (Figure 3C). The OI is in the range of 21 to 183 mg CO_2/g C_{org}, and production index (PI) values are as much as 0.07 (Figure 3E). The S_2 values range between 22 and 246 mg HC/g rock (Figure 3D). The T_{max} is in the range of 424 to 438°C (Figure 3E).

For the samples of the Loia Group in the Samba well, a wide variation in the HI values (Figure 3C) ranging from 430 to 965 mg HC/g rock, with a mean value of approximately 751 mg HC/g rock is typical (Figure 3C). The OI ranges from 22 to 135 mg CO_2/g C_{org}, with a mean value of 64 mg CO_2/g C_{org}. The T_{max} is in the range of 429 to 437°C, and PI values range from 0.01 to 0.05 (Figure 3E). Samples show various S_2 values in the range of 6 to 160 mg HC/g rock. For the Loia and Stanleyville groups, an increase of S_2 with increasing C_{org} is typical (Figure 3D). Another pattern is given for the samples of the Lukuga and Aruwimi groups. For the Lukuga Group, the T_{max} ranges between 427 and 437°C, with HI values from 18 to 265 mg HC/g rock, OI values between 20 and 154 mg CO_2/g C_{org}, and PI value as much as 0.5. The Lukuga coal sample has an HI of 200 mg HC/g rock and an OI of 38 mg CO_2/g C_{org}, with a T_{max} of 426°C and a PI of 0.03 (Figure 3C–E). Based on their very low S_2 values, most HI and T_{max} values are not reliable for the samples of the Aruwimi Group. The T_{max} values range from 416 to 450°C, with PI as much as 0.8. All Rock-Eval parameters are compiled in Table 1.

Organic Petrography

An overview of maturity distribution is provided by R_o data, which is considered to be the most reliable and most commonly used maturity indicator (Dow, 1977; Waples et al., 1992). However, most of the samples of the Congo Basin contain a large amount of resedimented vitrinite and vitrinite-like particles, especially Pennsylvanian–Lower Permian samples of the Lukuga Group in the Dekese well, and to a lesser extent, samples of the Walikale area. The dominance of resedimented particles suggests that Mississippian and possibly also Devonian rocks were deposited at the margin of the basin over much greater areas than those represented by the present-day outcrops. Erosion of these units at the basin margin occurred at the same time when Pennsylvanian to Lower Permian units were deposited in the basin center.

The R_o values of all samples are plotted in Figure 3F and in Table 1. The R_o measurements revealed values of 0.6 to 0.8% for the Lukuga Group (Dekese well; Figure 3F), where values increase with depth. However, much scatter exists because of the predominance of resedimented vitrinite,

Table 1. Overview of Elemental Analysis Data*

Sample No.	Location	Group/Unit	Depth (m)	C_{org} (%)	C_{inorg} (%)	$CaCO_3$ (%)	TS (%)	S_1 (mg/g)	S_2 (mg/g)	S_3 (mg/g)	T_{max} (°C)	OI (mg CO_2/ g C_{org})	HI (mg HC/ g C_{org})	PI (S_1/ S_1 + S_2)	R_o (%)
1234	Dekese	Loia/C	703.0	0.09	0.14	1.15									
304	Dekese		707.8	0.07	0.29	2.47									
305	Dekese	Lukuga/ D (Ecca)	712.0	0.16	6.31	52.59									
306	Dekese		723.0	0.10	0.90	7.50									
307	Dekese		726.0	0.12	0.70	5.87									
308	Dekese		732.0	0.06	0.73	6.16									
140	Dekese	Lukuga/ F-(Dwyka)	924.6	0.47	0.09	0.74									0.73
141	Dekese		924.9	0.46	0.11	0.94									0.64
151	Dekese		942.2	0.46	0.12	1.00									0.73
152	Dekese		942.9	0.53	0.13	1.07		0.03	0.1	0.8	427	154	18	0.3	0.74
153	Dekese		943.4	0.44	0.13	1.06									0.72
154	Dekese		944.4	0.50	0.16	1.29									0.77
1235	Dekese		993.5	0.49	0.11	0.92		0.04	0.1	0.7	432	31	156	0.2	0.84
1237	Dekese		1019.7	0.68	0.22	1.86	0.09	0.09	0.4	1	437	66	162	0.2	0.77
142	Dekese		1049.2	0.95	0.05	0.41		0.05	0.3	0.7	430	72	36	0.1	0.68
143	Dekese		1050.2	0.47	0.08	0.67									0.74
144	Dekese		1050.5	0.42	0.09	0.78									0.73
145	Dekese		1050.9	0.51	0.09	0.75		0.05	0.06	0.6	432	128	10	0.5	0.77
146	Dekese		1051.2	0.44	0.09	0.71									0.74
155	Dekese		1067.9	2.30	0.12	1.02		0.08	2	0.7	431	30	99	0.03	0.67
147	Dekese		1068.0	2.40	0.05	0.41		0.07	2	0.8	431	33	103	0.03	0.67
148	Dekese		1068.2	1.83	0.05	0.42	0.18	0.05	0.6	0.9	435	50	35	0.07	0.75
156	Dekese		1068.7	0.43	0.02	0.15									0.61
157	Dekese		1069.0	0.37	0.02	0.15		0.05	0.1	0.5		80	12	0.4	
149	Dekese		1069.9	0.63	0.03	0.27		0.05	0.2	0.5	430	77	27	0.2	0.68
158	Dekese		1095.3	0.64	0.13	1.07		0.04	0.2	0.1	431	22	33	0.1	0.7
159	Dekese		1096.0	0.61	0.07	0.58		0.07	0.3	0.4	430	60	36	0.2	0.7
160	Dekese		1098.0	0.73	0.12	1.02	0.15	0.06	0.3	0.7	434	69	32	0.1	0.67
150	Dekese		1099.3	0.72	0.14	1.18		0.05	0.4	0.9	432	99	39	0.1	0.6
161	Dekese		1134.2	0.97	1.02	8.52		0.07	0.2	0.7	432	101	28	0.3	0.56
162	Dekese		1136.7	0.95	0.09	0.75		0.07	0.4	0.78	431	80	41	0.1	0.59
163	Dekese		1136.8	0.70	0.15	1.27		0.04	0.2	0.5	432	38	86	0.16	0.61
164	Dekese		1138.9	0.97	0.12	0.97		0.04	0.2	0.5	430	40	100	0.15	
1238	Dekese		1189.9	0.55	0.14	1.12									

1236	Dekese		1259.8	0.62	0.15	1.27		0.08	0.3	0.4	438	47	65	0.22	0.7
1228	Dekese		1261.0	0.58	0.12	0.98		0.06	0.3		427	49		0.17	0.55
1232	Dekese		1312.3	0.15	0.35	2.90		0.04	0.2	0.8	427	36	188	0.21	0.74
1231	Dekese		1340.4	0.15	0.29	2.43									
1230	Dekese		1379.1	0.14	0.42	3.48		0.08	0.2	1	429	41	235	0.28	0.64
1225	Dekese		1459.0	0.42	0.09	0.74									0.68
1224	Dekese		1459.7	0.37	0.20	1.66									0.71
1227	Dekese		1501.5	0.51	0.06	0.47									0.74
165	Dekese		1530.0	0.43	0.07	0.57									0.67
166	Dekese		1530.8	0.30	0.02	0.18									0.74
167	Dekese		1531.4	0.36	0.03	0.25									
168	Dekese		1532.2	0.45	0.03	0.21									
169	Dekese		1532.5	0.42	0.06	0.47									
170	Dekese		1533.2	0.39	0.05	0.42									
171	Dekese		1533.5	0.41	0.12	1.02									
1226	Dekese		1549.0	0.11	0.54	4.54									
1229	Dekese	Lukuga/ G (Dwyka)	1661.5	0.06	0.35	2.94									
172	Aruwimi River, Malili-Banalia section	Aruwimi/ Upper Alolo		0.13	3.16	26.35									
173				0.17	3.36	28.03									
174				0.18	0.19	1.55									
175				0.26	2.97	24.71									
176				0.07	0.06	0.53									
177		Aruwimi/ Middle Alolo		0.18	1.66	13.82		0.12	0.03	0.3	416	16	2	0.8	
178		Aruwimi/ Lower Alolo		0.18	0.12	1.00		0.1	0.01	0.8		1	78		
179				0.05	0.06	0.50		0.1	0.2	0.5	442	38	113	0.45	
180				0.04	0.05	0.46		0.1	0.02			1			
181				0.09	5.91	49.26		0.1	0.8		430	93		0.1	
309	Aruwimi River, Yambuya section	Aruwimi/ Alolo		1.82	0.110	0.92	2.07								
310				0.18	9.777	81.45									
311				0.27	7.956	66.27									
312				0.24	9.542	79.48									
313				0.17	8.77	73.07									

Table 1. Continued

Sample No.	Location	Group/Unit	Depth (m)	C_{org} (%)	C_{inorg} (%)	$CaCO_3$ (%)	TS (%)	S_1 (mg/g)	S_2 (mg/g)	S_3 (mg/g)	T_{max} (°C)	OI (mg CO_2/g C_{org})	HI (mg HC/g C_{org})	PI (S_1/S_1 + S_2)	R_o (%)
1250	Pont de la Lindi	Aruwimi/Alolo		0.22	5.04	41.94									
1251				0.12	6.42	53.50									
1252				0.27	2.16	17.98									
1253				0.09	2.99	24.91									
182	Aruwimi River, Bombwa region	Lokoma/Mamungi		0.06	2.46	20.47									
183				0.13	3.17	26.37									
184				0.07	0.18	1.50									
185				0.08	2.19	18.21									
186				0.08	3.69	30.77									
187				0.07	0.09	0.71									
188				0.06	0.09	0.71									
189				0.06	2.52	21.00									
190	Ituri River, between Penge and Avakubi	Ituri/Lenda		0.16	11.8	98.50									
191				0.15	10.4	87.00									
192				0.06	9.80	81.64									
193				0.08	0.01	0.10									
194				0.12	5.64	46.98									
195				0.11	10.6	88.91									
1239	Aruwimi River, Yambuya section	Aruwimi/Alolo		1.08	0.09	0.77									
1240				0.45	9.21	76.71									
1241				0.29	8.22	68.43									
1242				1.39	0.11	0.93	2.77								
1243				0.89	0.11	0.91	4.43								
1244				0.25	7.32	60.99									
1245				0.40	8.75	72.88		0.1	0.06	0.8		15	200		
1246				1.11	0.11	0.88	2.99	0.01	0.02	3		2	277		
1247				0.36	9.24	76.95									

1248				0.37	7.64	63.63									
1249				0.30	11.1	92.74									
1250	Pont de la Lindi	Aruwimi/ Alolo		0.22	5.04	41.94									
1251				0.12	6.42	53.50									
1252				0.27	2.16	17.98									
1253				0.09	2.99	24.91									
1254	Ubangi, Yakoma	U. Lokoma (Bombua)/ Mamungi		0.05	3.68	30.61									
1255	Ubangi			0.11	3.35	27.92									
1256	Ubangi, Yakoma			0.12	2.39	19.86									
1257	Ubangi, Gbadolite			0.06	0.02	0.15									
1258	Ubangi, Dondo			0.05	0.01	0.12									
1259	Ubangi			0.19	2.20	18.33	2.69								
1260	Ubangi			0.04	0.02	0.18									
1261	Ubangi			0.20	3.62	30.12									
1262	Ubangi, Dondo			0.14	0.26	2.13									
1263	Walikale	Lukuga/W3 (Upper Dwyka)		0.43	0.18	1.53		0.04	0.2	0.5	437	40	111	0.19	
1269	Walikale			0.54	0.14	1.15		0.04	0.2	1	436	37	258	0.17	0.71
1270	Walikale			0.41	0.11	0.87		0.02	0.1	1	438	20	265	0.2	
1271	Walikale			0.61	0.18	1.47		0.1	0.3	1	436	48	208	0.15	0.70
1268	Walikale			0.21	0.08	0.63									
1264	Walikale			0.65	0.20	1.65	0.07	0.1	0.3	0.2	436	52	37	0.11	0.69
1267	Walikale			1.32	0.25	2.04	0.08	0.1	1	0.6	438	90	51	0.07	0.71
1265	Walikale			0.92	0.26	2.17	0.11	0.1	0.7	0	439	80		0.1	
1266	Walikale			0.30	0.15	1.21									
127	Walikale			0.08	11.67	97.20									
299	Samba	Loia	567.8	0.380	1.261	10.51									
300	Samba	Loia	632.8	0.145	1.027	8.56									
301	Samba	Loia	657.1	19.38	0.36	3.00	3.83	3	159	161	435	821	135	0.02	0.56
292	Samba	Loia	665.2	11.01	2.09	17.41	0.58	2	79	4	431	717	36	0.02	
293	Samba	Loia	676.2	1.23	0.61	5.10	1.82	0.3	6	2	429	503	128	0.05	
302	Samba	Loia	706.4	1.238	0.037	0.30		0.1	8	0.7	433	663	59	0.01	

Table 1. Continued

Sample No.	Location	Group/Unit	Depth (m)	C_{org} (%)	C_{inorg} (%)	$CaCO_3$ (%)	TS (%)	S_1 (mg/g)	S_2 (mg/g)	S_3 (mg/g)	T_{max} (°C)	OI (mg CO_2/ g C_{org})	HI (mg HC/ g C_{org})	PI (S_1/ S_1 + S_2)	R_o (%)
303	Samba	Loia	757.0	3.88	0.76	6.34	3.12	1	36	2	430	917	68	0.03	0.65
294	Samba	Loia	763.5	1.05	3.12	25.96		0.2	6	0.8	432	630	82	0.03	
295	Samba	Loia	781.0	5.85	1.51	12.55		2	55	1	437	937	22	0.04	
296	Samba	Loia	825.3	1.60	2.40	20.03		0.3	14	0.9	436	894	59	0.02	0.70
1202	Samba	Loia	734.9	2.91	0.46	3.82	1.47	1	32	0.8	430	430	27	0.04	
1203	Samba	Loia	734.9	4.51	1.17	9.73		2	42	4	429	921	103	0.05	
1201	Samba	Loia	734.9	8.78	1.05	8.71	2.15	3	72	3	433	825	31	0.03	
1205	Samba	Loia	739.7	3.95	1.53	12.70	0.59	2	38	2	432	965	39	0.04	
1204	Samba	Loia	739.8	4.67	0.29	2.45	1.23	2	41	2	425	873	47	0.05	
1200	Samba	Stanleyville	1008.6	1.50	0.11	0.95									
1198	Samba	Stanleyville	1008.6	0.20	1.98	16.46									
1197	Samba	Stanleyville	1008.6	0.54	2.10	17.52									
1199	Samba	Stanleyville	1008.6	0.14	2.53	21.07									
297	Samba	Stanleyville	1011.2	0.13	0.91	7.58									
298	Samba	Stanleyville	1031.5	0.09	1.81	15.10									
1206	Samba	Aruwimi	1856.6	0.06	0.70	0.76									
314	Congo Coal Field	Lukuga		47.65	0.38	3.17	0.51	3	97	18	426	38	204	0.03	0.47
315	Lualaba	Stanleyville/ Waniarukula		2.66	10.24	85.36	0.42	1	22	76	434		812	0.04	0.41
316	Lualaba	Stanleyville/ Kewe Village		4.68	7.78	64.82	0.42	1	37	85	428		786	0.04	0.47
317	Lualaba	Stanleyville/ Oviataku		13.15	2.44	20.33	0.46	6	124	3	426	21	943	0.05	0.55
318	Lualaba	Stanleyville/ Bendera Village		8.49	4.79	39.95	0.21	4	87	15	435	183	1028	0.04	0.50
319	Lualaba	Stanleyville/ Songa_Kewe		25.43	0.85	7.08	0.63	6	246	7	438	26	969	0.02	0.55
320	Lualaba	Stanleyville/ Lilu Valley		10.56	3.60	29.99	0.30	7	97	4	424	36	914	0.07	0.55

*(Corg: total organic carbon; Cinorg: inorganic carbon; CaCO3: calcium carbonate in percent ; TS: total sulfur in percent), Rock-Eval pyrolysis (Rock-Eval-hydrogen index (HI), and oxygen index (OI), Rock-Eval production index (PI) (S_1/S_1 + S_2), and T_{max} (heating temperature at which peak of S_2 Occurs), and vitrinite reflectance data of selected samples from the Central Congo Basin.

which is difficult to distinguish from autochthonous vitrinite. The Kalemie coal sample microscopically presents a high amount of vitrinite and sporinite, the latter with a greenish to yellow fluorescence. Alginite was also observed but only in minor amounts. The R_o of this outcrop coal sample is 0.47% (Figure 3F; Table 1).

The R_o values of samples of the Stanleyville Group in the Lualaba Basin range from 0.4 to 0.55% (Figure 3F; Table 1), whereas samples of the Loia Group (Samba well) show R_o values ranging from 0.56 to 0.7%. The latter samples represent less abundant vitrinite and vitrinitelike particles but lamalginite as a predominant maceral (as much as 90%). Fluorescence observations revealed a greenish to yellow color of the particles. Fresh pyrite was also abundant in the samples of the Loia Group, which revealed a nearly unweathered kind of the sample material (Littke et al., 1991b).

Molecular Organic Geochemistry

All of the investigated samples of the Congo Basin contain n-alkanes in the range of n-C_{12} to n-C_{31} (Figure 4; Table 2). In most samples, a clear dominance of short-chain n-alkanes (n-C_{15}–n-C_{19}) relative to long-chain n-alkanes (n-C_{27}–n-C_{31}) is not obvious, indicating moderate to low maturity levels and a mixture of aquatic (lacustrine or marine) and terrestrial OM. At high levels of maturity, long-chain n-alkanes are cracked and short-chain n-alkanes clearly predominate. Very high n-C_{17}/n-C_{27} ratios (>10) were only recorded for the Aruwimi sample and one of the Lukuga samples. The ratio of n-C_{17} to n-C_{27} is less than 1 in samples of the Loia Group and in some samples of the Lukuga Group; in all other samples, it is more than 1, with the highest dominance of n-C_{17} in the Aruwimi Group. The abundance of pristine (Pr) and phytane (Ph) is moderate to high, with a weak dominance of Pr in samples of the Aruwimi, Lukuga, and Stanleyville groups. In samples of the Loia Group, a dominance of Ph could be observed, which is typical of source rocks deposited under anoxic conditions and/or carbonate to evaporite environments. The latter can, however, be excluded because of the low to moderate carbonate contents of Loia sediments. The ratios of Pr/n-C_{17} and Ph/n-C_{18} range from 0.4 and 1.4, respectively, with the coal sample reaching a value of 3.8 (Figure 5). Different ratios were used to calculate the ratio of odd-carbon-numbered over even-carbon-numbered n-alkanes (carbon preference index [CPI] and odd-to-even predominance [OEP]; Table 3). High values are typical for the Lukuga samples, including the coal from Kalemie, indicating a strong terrestrial contribution in this unit. The Loia and Stanleyville samples show lower values, but—with one exception—also predominance of odd-numbered n-alkanes. Lower values were recorded for Aruwimi samples, which were deposited before the appearance of terrestrial plants.

Biomarker ratios were used to characterize the depositional environment and the maturation range of potential source rocks. The biomarkers we evaluated for this study were tricyclic and pentacyclic triterpanes as well as steranes and diasteranes (cf. Peters and Moldowan, 1991), with a focus on evaluation of peak area ratios from tricyclic and pentacyclic terpanes measured from the M/Z 191 trace, steranes measured from the M/Z 217 and 218 trace, and diasteranes from the M/Z 259 trace (Table 2; Figure 6). In addition, sesquiterpanes and tetracyclic terpanes were found in some samples, but only in minor amounts.

For the tetracyclic terpanes, only $C_{23}H_{40}$ was identified in all samples, $C_{24}H_{42}$ in addition was identified only for one Lukuga sample from the Walikale area (1267). Tricyclic terpanes in the range of C_{19} to C_{25} were abundant, whereas C_{26} and larger carbon numbers were mainly under the detection limit, except in samples 1204 and 1205 (Loia Group). Identification of these tricyclic terpanes was based on peak identification described by Wang (1993). For the Lukuga coal sample, only $C_{20}H_{36}$ molecules could be identified. Dominant peaks in the samples of the Lukuga and Loia groups are the $\alpha\alpha$ and $\beta\alpha$ configurations. The ratio tricyclics/17α-hopanes, which is helpful to describe the maturity range, was used for the Loia samples, which revealed values between 0.17 and 0.44 (Table 3). Pentacyclic terpanes of the hopane series from C_{27} to C_{32} are dominated by C_{29} hopane and C_{30} to C_{31} hopanes, with only a

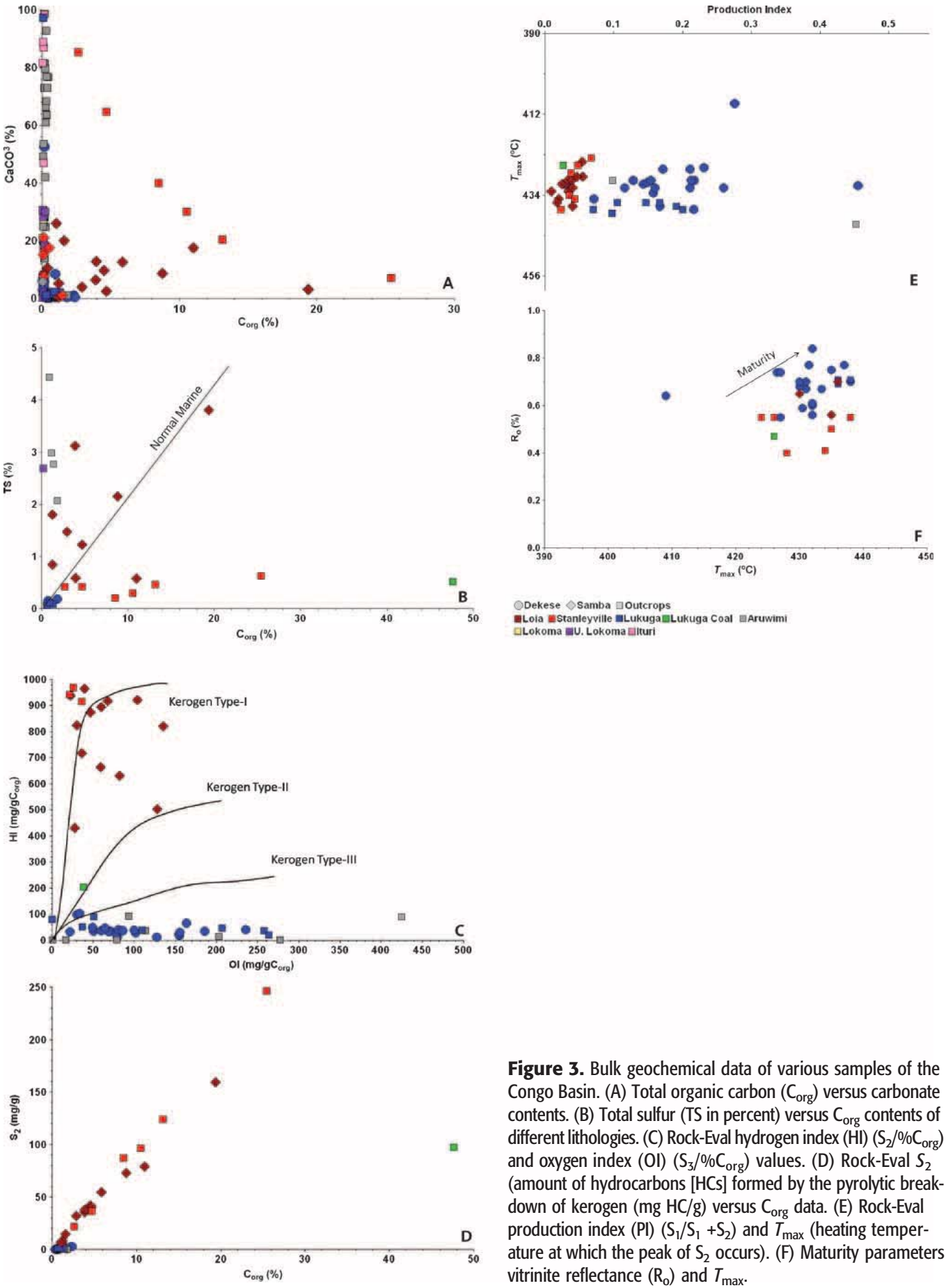

Figure 3. Bulk geochemical data of various samples of the Congo Basin. (A) Total organic carbon (C_{org}) versus carbonate contents. (B) Total sulfur (TS in percent) versus C_{org} contents of different lithologies. (C) Rock-Eval hydrogen index (HI) (S_2/%C_{org}) and oxygen index (OI) (S_3/%C_{org}) values. (D) Rock-Eval S_2 (amount of hydrocarbons [HCs] formed by the pyrolytic breakdown of kerogen (mg HC/g) versus C_{org} data. (E) Rock-Eval production index (PI) (S_1/S_1 +S_2) and T_{max} (heating temperature at which the peak of S_2 occurs). (F) Maturity parameters vitrinite reflectance (R_o) and T_{max}.

minor contribution of C_{32} homohopanes. The 17α(H)21β(H) and 17β(H)21α(H) isomers dominate the M/Z 191 fragmentograms. The C_{30} to C_{31} hopanes were present in both the Loia and Lukuga groups and in the Lukuga coal sample. The norhopane (C_{29})/hopane (C_{30}) ratio is less than 0.5 in all samples, except in the Lukuga samples, where it is 0.8 for the coal sample and 1.1 for sample 1267. The C_{32} 22S/(22S + 22R) ratio ranges between 0.23 and 0.56. The T_m (C_{27} 17α[H]-22,29,30-trisnorhopane) is more dominant than T_s (C_{27} 18α[H]-22,29,30-trisnorneophane) in all samples. The ratio of $T_s/(T_s + T_m)$ is in all samples less than 0.5 and only in the Loia samples slightly higher (0.52; Table 3). The ratios of C_{31}/C_{30} hopane with values less than 0.3, for all samples, indicate lacustrine instead of marine source rock depositional environments. The terpane assignments are given in Table 2, and characteristic chromatograms are shown in panels A to C, G, and H of Figure 6. Table 3 summarizes the hopane ratios.

The C_{29} 20S/(20S + 20R) ratios range between 0.1 and 0.55, with highest values for the Lukuga Group, especially the Lukuga coal sample. High concentrations of 24-ethyl-5α, 14α, 17α(H)-cholestane occur in all samples, 24-methylcholestanes being dominant especially in samples of the Loia Group. Measurements of C_{27}, C_{28}, and C_{29} revealed a dominance of the C_{29} steranes. Sterane and assignments are given in Table 2 and characteristic chromatograms in panels D to F of Figure 6. Table 3 and Figure 7 summarize the sterane ratios. Diasteranes, which are used for maturity evaluation, could only be identified for one sample of the Lukuga Group (1267). The diasteranes/steranes ratio revealed for this sample a value of 0.31, the ratio of 20S/(20S + 20R)13β,17α(H)-diasteranes is 0.6. The sterane/hopane ratio calculated for the Loia and Lukuga groups revealed values between 0.09 and 1.17, with highest values for the Loia Group.

Numerical One-Dimensional Modeling, Dekese Well

All information as stratigraphic intervals and thicknesses concerning the Dekese well was adopted from the "Description du Sondage de Dekese" (Cahen et al., 1960). Additional data on the paleogeographic history of the area from (Daly et al., 1992; Giresse, 2005) were also used. For the Dekese well, a marked phase of subsidence was assumed for the Late Cretaceous (Cenomanian–Santonian) with deposition of approximately 1000 m (~3280 ft) of sediments (Figure 8A).

Calibration of this model was performed using measured R_o data from the Lukuga Group. The calculated and measured R_o data are shown in Figure 8B. The coalification was calibrated with the measured R_o data, leading to the assumption of (1) a heat flow of 68 mWm^{-2} at the time of maximum burial (80 Ma) (Figure 8C) and (2) a deposited and then eroded thickness of Upper Cretaceous sequences of 1000 m (3280 ft).

The maturation, burial, and heat-flow histories of the Dekese well are shown in panels A to E of Figure 8. The burial history shows one significant phase of subsidence (120–90 Ma). After the deposition of Paleozoic layers with a maximum thickness of 3000 m (9840 ft), rapid and important subsidence occurred in the middle of the Late Cretaceous. The depth of the deepest horizon taken into account in the model (Ituri) rapidly increased as much as approximately 4850 m (15,912 ft) within 11 m.y. At that time, the base of the Lukuga Group, for which calibration data are available, reached a depth of approximately 2600 m (~8530 ft). After deposition of approximately 900 m (~2950 ft) of Pennsylvanian–Lower Permian sediments of the Lukuga Group, several hundred meters of sediments were eroded during Middle Permian uplift. Note that no exact conclusion on eroded thicknesses and heat flows for this period can be deduced from our data, but temperatures were definitely lower than those later reached during the Cretaceous. Therefore, a very high heat flow and an erosion of several thousand meters can be excluded. Jurassic and Lower Cretaceous sediments accumulated to a thickness of a few hundred meters. The base of the Lukuga Group stayed at approximately 1000 m (~3280 ft) deep. This was followed by rapid deposition of almost 2000 m (6562 ft) of sediments, the base of Ituri and Lukuga groups reaching depths of 4850 and 2600 m (15,912 and 8530 ft), respectively.

Maximum burial was reached at approximately 80 Ma (Santonian–Campanian transition), during which the base of the Ituri and Lukuga groups reached 175 and 110°C, respectively, leading to corresponding maturities of 1.8 and 0.8% (Figure 8D, E). The maturity level remained constant from the Late Cretaceous until the Holocene. Note that calibration data also allow the assumption of a lower heat flow during maximum burial; in this case, a higher eroded thickness has to be assumed. In other words, the amount of erosion (1000 m [3280 ft]) is regarded as a minimum.

Numerical One-Dimensional Modeling, Samba Well

All information as stratigraphic intervals and thicknesses concerning the Samba well was adopted from Cahen et al. (1959). Additional data of the paleogeographic history of the area were also used (Daly et al., 1992; Giresse, 2005). Similarly, as for the Dekese well, a marked phase of subsidence was assumed for the Late Cretaceous (Cenomanian–Santonian), with rapid deposition and erosion of approximately 900 m (~2950 ft) of sediments (Figure 9A).

Calibration of this model was performed with assistance of the measured R_o data. The calculated and measured R_o data are shown in Figure 9B. The coalification was calibrated with the measured R_o data and led to an (1) assumed heat flow of 72 mWm^{-2} for the time of maximum burial (80 Ma) (Figure 9C) and an (2) assumed deposited and eroded thickness of the Kwango Group of 900 m (2950 ft) (Figure 9A). Today, this sequence is almost completely eroded, leaving only 115 m (377 ft) in the well. The burial history shows one significant main phase of subsidence that started in the Late Jurassic to Early Cretaceous and shifted the base of the Aruwimi red beds to a depth of approximately 2850 m (~9230 ft). For the sediments of the Stanleyville Group, a depth of 2000 m (6562 ft) could be calculated. At this time, the base of the Loia Group, for which calibration data are available, reached a depth of approximately 1600 m (5250 ft). After deposition of these layers and the sediments of Bokungu Group, rapid deposition led to a maximum burial depth of 1800 m (5906 ft) and temperatures of approximately 100°C for the base of the Loia Group. This was followed by erosion of the Kwango Group because of uplift that led to a present-day depth of 1200 m (3937 ft) for the base of the Stanleyville Group, and 900 m (2950 ft) for the base of the Loia Group. Note that calibration data also allow the assumption of a lower heat flow during maximum burial; in this case, a higher eroded thickness has to be assumed. Thus, the amount of erosion (~900 m [~2950 ft]) is regarded as a minimum.

Maximum burial was reached at 80 Ma, and the base of the Aruwimi Group reached temperatures as much as 130°C, leading to a corresponding maturity of 0.8% R_o. The Stanleyville Group reached, at the maximum burial, a temperature of 120°C (Figure 9E). This value corresponds to a calculated maturity value of 0.7% R_o (Figure 9D). From the Late Cretaceous until the present day, the maturity remained stable and present-day temperatures are at approximately 80°C.

DISCUSSION

Depositional Environment

The high $CaCO_3$ contents of the samples of the Ituri Group suggest a strong marine or lacustrine influence; OM could not be identified because of the low C_{org} contents. The Lokoma Group contains low amounts of $CaCO_3$. The Aruwimi Group contains marine aquatic OM in very low quantities and commonly moderate carbonate contents, suggesting a marine depositional environment with a high influence of terrestrial OM. Type III to IV kerogen indicates the presence of highly inert material that has been affected by a moderate to high thermal maturity.

Samples of the Lukuga Group revealed a high amount of terrestrial-derived OM, represented by type III to IV kerogen. The low contents of carbonate lead also to the assumption of a terrestrial, more oxic, depositional environment. The investigated coal sample of the Lukuga Group is a quite typical mineral-enriched coal with abundant vitrinite

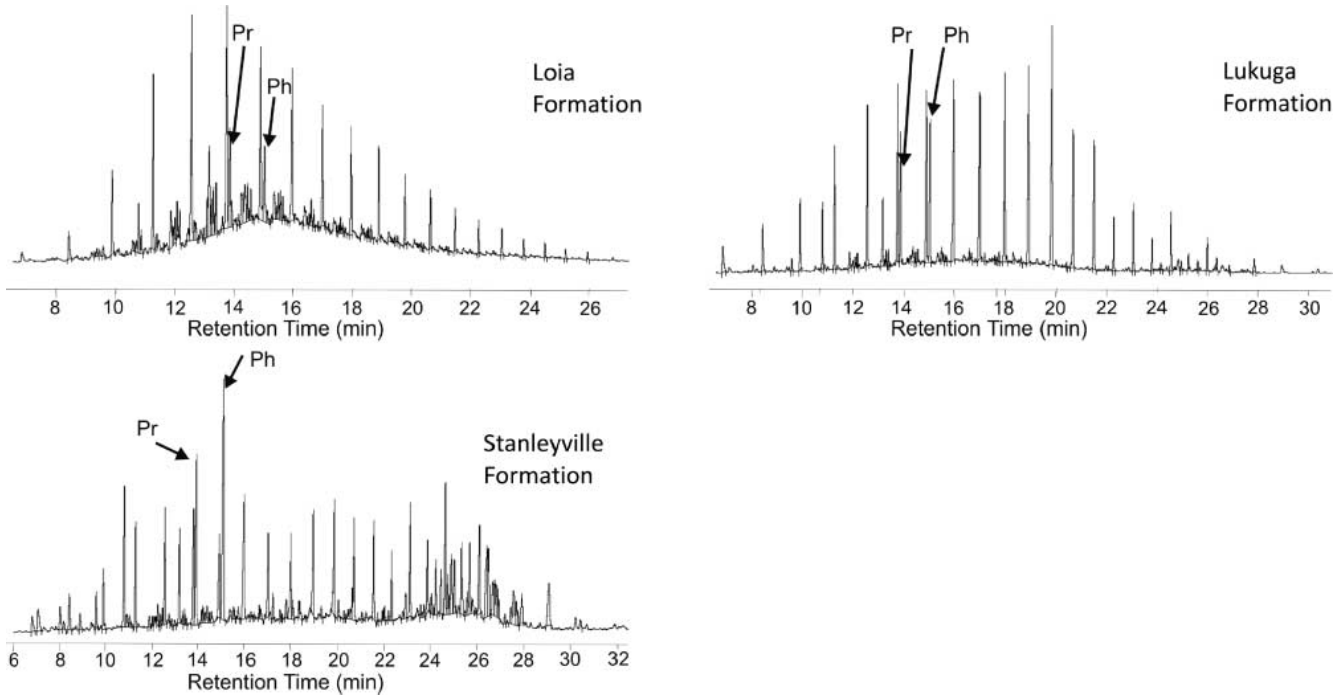

Figure 4. The *n*-alkane distribution pattern for representative samples of Loia, Lukuga, and Stanleyville groups. Pr = pristane; Ph = phytane.

and sporinite. It probably derives from peat deposited in a wet topogenous swamp.

The Stanleyville Group revealed a highly variable carbonate content. Samples representing type I kerogen revealed the lowest carbonate contents. This leads to the assumption of an aquatic (most likely lacustrine) depositional environment, but with a strong (periodic) influence of terrestrial OM. The depositional environment is described by Lepersonne (1977) as dominantly shallow lacustrine to swampy and even brackish, partly in relatively arid climate for the upper part of the Stanleyville Group. A thin calcareous level found at Songa (south of Lubumbashi) was considered as marine on the basis of fossil fishes attributed to a marine species, but a recent revision (L. Taverne, 2011, personal communication) shows that this ichtyofauna is highly endemic and exists in both marine and continental environments. In the absence of clear indications for a marine connection at that time and because of the location of the site in the middle of the Gondwana continent, deposition of the Stanleyville Group under lacustrine conditions is most likely. Samples of the Loia Group show high C_{org} values with low to moderate carbonate contents, indicating a more oxic depositional environment.

The TS values were measured in some samples to provide an insight into the depositional environment and, in particular, to the intensity of bacterial sulfate reduction (Berner, 1970, 1984). Under anoxic conditions, dissolved sulfate is reduced to H_2S, which reacts with iron minerals to form iron sulfides. The TS/C_{org} ratios reflect the intensity of microbial sulfate reduction in OM decomposition, giving a qualitative indication of the redox status in the depositional environment. Berner (1970, 1984) found an empirical relationship between sulfur content and C_{org} content, which is typical for most marine sediments deposited under aerobic bottom waters (Figure 3B).

Moderate to high sulfur content and TS/C_{org} values (Figure 3B) are characteristic of nearly all samples of the Loia, Aruwimi, and Lokoma groups. These moderate to high ratios indicate a generally strong bacterial sulfate reduction. Very high TS/C_{org} values suggest that more OM is consumed via sulfate reduction than under normal marine conditions (Berner, 1984). Visual analysis indicates the presence of significant amounts of pyrite in the

Table 2. Identified Tricyclic Terpanes, Hopanes, and Steranes

Tricyclic Terpanes (M/Z 191)	
a	13β (methyl)-Tricyclic terpane $C_{19}H_{34}$
b	13β, 14β-Tricyclic terpane $C_{20}H_{36}$
c	13α, 14β-Tricyclic terpane $C_{20}H_{36}$
d	13β, 14α-Tricyclic terpane $C_{20}H_{36}$
e	13α, 14α-Tricyclic terpane $C_{20}H_{36}$
f	13β, 14β-Tricyclic terpane $C_{21}H_{38}$
g	13α, 14β-Tricyclic terpane $C_{21}H_{38}$
h	13β, 14α-Tricyclic terpane $C_{21}H_{38}$
i	13α, 14β-Tricyclic terpane $C_{21}H_{38}$
j	13β, 14α-Tricyclic terpane $C_{22}H_{40}$
k	13α, 14β-Tricyclic terpane $C_{22}H_{40}$
l	13β, 14α-Tricyclic terpane $C_{23}H_{42}$
m	13α, 14α-Tricyclic terpane $C_{20}H_{36}$
n	13β, 14α-Tricyclic terpane $C_{24}H_{44}$
o	13α, 14α-Tricyclic terpane $C_{24}H_{44}$
p	Tetracyclic Terpane $C_{23}H_{40}$
q	13β, 14α-Tricyclic terpane $C_{25}H_{46}$
r	13α, 14α-Tricyclic terpane $C_{25}H_{46}$
s	Tetracyclic Terpane $C_{24}H_{42}$
t	13β, 14α-Tricyclic terpane $C_{26}H_{48}$
u	13β, 14α-Tricyclic terpane $C_{26}H_{48}$
v	13α, 14α-Tricyclic terpane $C_{26}H_{48}$
Hopanes (M/Z 191)	
1	18α(H)-22,29,30-Trisnorneohopane (T_s)
2	17α(H)-22,29,30-Trisnorhopane (T_m)
3	17α(H), 21β(H)-28,30-bisnorhopan
4	17α(H),21β(H)-30-Norhopane
5	17β(H),21β(H)-30-Norhopane
6	17α(H),21β(H)-Hopane
7	17β(H),21α(H)-30-Norhopane
8	17β(H),21α(H)-Hopane
9	(22S)-17α(H),21β(H)-29-Homohopane
10	(22R)-17α(H),21β(H)-29-Homohopane
11	17β(H), 21β(H)-Homohopane
12	17β(H), 21β(H)-hopane
13	(22S)-17α(H),21β(H)-29-Dihomohopane
14	(22R)-17α(H),21β(H)-29-Dihomohopane
Steranes (M/Z 217 and 218)	
A	(20S)-5α(H),14α(H),17α(H)-Cholestane
B	(20R)-5α(H),14α(H),17α(H)-Cholestane
C	(20S)-24-Methyl-5α(H),14β(H),17β(H)-Cholestane
D	(20R)-24-Methyl-5α(H),14β(H),17β(H)-Cholestane
E	(20S)-24-Methyl-5α(H),14α(H),17α(H)-Cholestane
F	(20S)-24-Ethyl-5α(H),14α(H),17α(H)-Cholestane
G	(20R)-24-Ethyl-5α(H),14β(H),17β(H)-Cholestane
H	(20S)-24-Ethyl-5α(H),14β(H),17β(H)-Cholestane
I	(20R)-24-Ethyl-5α(H),14α(H),17α(H)-Cholestane

samples of the Aruwimi Group derived from bacterial sulfate reduction and OM oxidation. This shows that sufficient iron was available to fix most of the sulfur in the form of iron sulfide. Interestingly, very high TS/C_{org} values are also typical for the Aruwimi sediments, but at low C_{org} values and also low HI values. The latter indicates only poor preservation of the primary OM, that is, no anoxic bottom water. Another explanation for the high TS/C_{org} values in these sediments would be a petroleum impregnation, followed by (bacterial) sulfate reduction and petroleum oxidation. However, allochthonous solid bitumen was not observed in the samples.

Littke et al. (1991a) and Lückge et al. (1996) showed that the consumption of part of the metabolized OM during early diagenesis greatly influenced the quality of OM in shallow-marine sediments. The bulk of the Loia samples shows high C_{org} and TS contents, but only moderate TS/C_{org} values. This might indicate that these samples were deposited under high productivity conditions, with bottom waters that were not anoxic, but only partly reduced in molecular oxygen. Thus, sulfur uptake into the sediments occurred only in the freshly deposited sediment, probably at a few decimeters below the sediment and water interface. In completely anoxic waters, sulfide precipitation and sulfur uptake into OM already starts within the water column, leading to high TS/C_{org} values (Sinninghe Damsté and Köster, 1998). In contrast, the samples of the Stanleyville Group revealed high amounts of C_{org} but only low to moderate sulfur contents. This could be related to a strong weathering of these rocks that causes an oxidation of sulfides (pyrite) (Littke et al., 1991b).

The Lukuga Group was deposited under terrestrial conditions, as also supported by low TS values and TS/C_{org} ratios. The Lukuga coal sample revealed a low TS/C_{org} ratio (0.01), indicating a low consumption of sulfur in OM and, therefore, deposition under oxic terrestrial conditions. Based on the relationship between C_{org} and TS contents, the original sediment composition (original OM, carbonate, silicate) before sulfate reduction was calculated (Figure 10) (Littke, 1993).

As dissolved sulfate is reduced, the sulfide concentration in sediments increases, and part of the

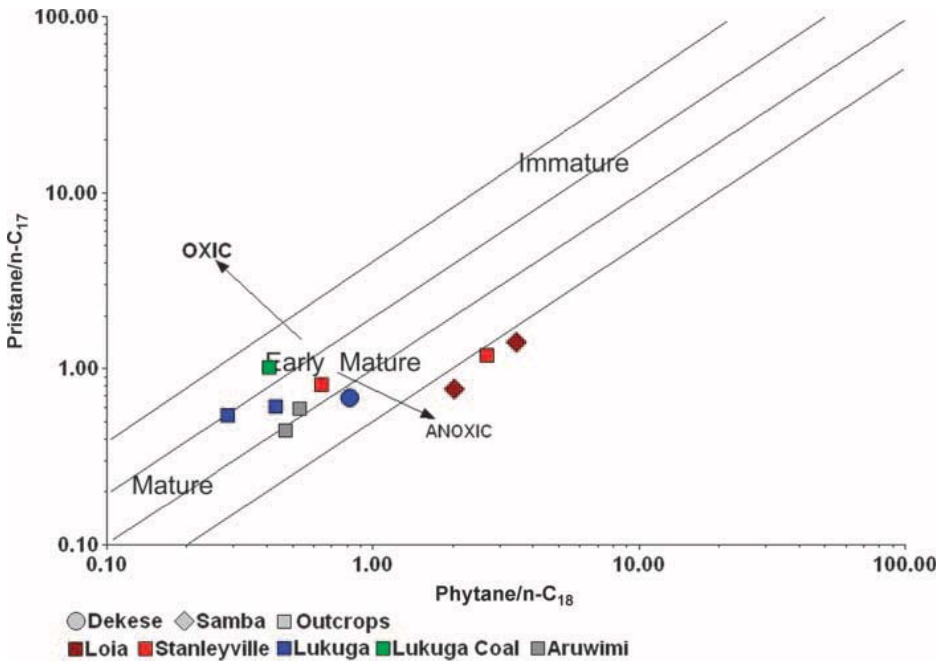

Figure 5. Pristane/n-C_{17} versus phytane/n-C_{18} for selected Congo samples (interpretation scheme according to Shanmungam, 1985).

C_{org} is consumed (Lallier-Vergès et al., 1993; Lückge et al., 1996). Sulfur concentration, therefore, can be used to calculate the OM content before sulfate reduction according to Littke (1993) (Figure 10). Samples from the Stanleyville Group define trends showing that, with an increase in silicate, the content of OM also increases. This tendency is explained as a consequence of a higher nutrient supply when the supply of clastic material increased in otherwise carbonate-dominated environments (Stein and Littke, 1990; Thurow et al., 1992).

The samples of the Loia Group represent another system, with a high percentage of silicate and an increasing amount of OM with a decrease in silicate (Figure 10). The high amount of OM reflects high bioproductivity caused by a change from terrestrial to aquatic influences or a higher amount of preservation possibly caused by anoxic to dysoxic water conditions. Samples of the Aruwimi and Lukuga groups did not reveal a particular trend. They contain a high amount of silicate with only low to moderate amounts of OM and carbonate. This points to a highly terrestrial environment or to an aquatic, completely oxic environment, in which almost no OM was preserved.

Microscopic observations and n-alkane patterns show that the Loia and Stanleyville groups contain a mixture of predominant algal-derived and aquatic OM and minor terrestrial OM at variable carbonate contents. The Pr/n-C_{17} and Ph/n-C_{18} ratios are typical of an anoxic depositional environment (Figure 5).

Detailed biomarker analysis was done for some samples of the Loia and Lukuga groups, which seem to be hardly affected by weathering. Both sample sets revealed contributions of tricyclic terpanes in the range of C_{20} to C_{25}. These are typically evidence of a contribution from higher plant materials (Tissot and Welte, 1984). The occurrence of triterpanes reflects the contribution of prokaryotic membranes that are present in bacteria and blue-green algae (Tissot and Welte, 1984; Moldowan et al., 1985), whereas steranes originate from algae and higher land plants. The contribution of C_{30} to C_{31} hopanes in samples of the Loia and Lukuga groups is regarded as an indicator of deposition under more oxic conditions because otherwise, under highly reducing conditions, extended homohopanes should be present (Peters and Moldowan, 1991; Tyson and Pearson, 1991).

The dominance of C_{29} norhopane in the Lukuga Group, as a result of preferential preservation in the presence of sulfur, is frequently observed in sediments with limited iron availability such as carbonates (Blanc and Connan, 1992) and points to an oxic character of the sediments. The oxic character is also supported by the C_{31}/C_{30} hopane

Table 3. Biomarker Parameters (Pr: Pristane; Ph: Phytane; CPI: Carbon Preference Index; OEP: Odd-even Predominace)

Sample No.	Group; Well	Unit	Pr/ Ph	n-C_{17}/ n-C_{27}	CPI (Bray and Evans, 1961)	CPI (Philippi, 1965)	OEP	T_s/ (T_s + T_m)	Norhopane (C_{29})/ hopane (C_{30})	C_{32} 22S/ (22S + 22R)	C_{31} 22R/ C_{30}	C_{29} 20S/ (20S + 20R)	Steranes/ Hopanes	Tricyclic/ 17α-hopane
155	Lukuga; Dekese	F (Dwyka)	1.35	2.16	1.64	3.4	3.24	N/A	N/A	N/A	N/A	N/A	N/A	N/A
147	Lukuga; Dekese	F (Dwyka)	0.81	2.96	1.60	2.88	2.79	N/A	N/A	N/A	N/A	N/A	N/A	N/A
162	Lukuga; Dekese	F (Dwyka)	N/A	0.70	N/A	N/A	N/A	N/A	N/A	N/A	N/A	N/A	N/A	N/A
1240	Aruwini	Alolo	1.25	12.64	1.00	1.13	1.16	N/A	N/A	N/A	N/A	N/A	N/A	N/A
1242	Aruwini	Alolo	N/A	N/A	N/A	N/A	N/A	N/A	N/A	N/A	N/A	N/A	N/A	N/A
1264	Lukuga	W3 (Upper Dwyka)	1.88	10.35	N/A	N/A	N/A	N/A	N/A	N/A	N/A	N/A	N/A	N/A
1267	Lukuga	W3 (Upper Dwyka)	1.73	5.51	1.25	1.75	1.84	0.14	1.1	0.56	0.31	0.47	0.1	N/A
301	Loia; Samba		N/A	N/A	N/A	N/A	N/A	0.52	0.24	0.49	0.18	0.28	0.39	0.24
303	Loia; Samba		0.37	0.93	1.53	1.91	1.93	0.51	0.34	0.23	0.14	0.11	0.48	0.44
1204	Loia; Samba		0.58	1.3	1.44	1.6	1.55	0.30	0.24	0.37	0.19	0.19	0.54	0.17
1205	Loia; Samba		N/A	N/A	N/A	N/A	N/A	0.37	N/A	0.23	N/A	0.24	1.17	N/A
314	Lukuga; Coal Field	Coal seam	3.81	0.65	2.84	2.99	3.30	0.43	0.8	0.32	0.29	0.55	0.09	N/A
315	Stanleyville	Waniarukula	1.14	5.45	0.83	1.91	1.83	N/A	N/A	N/A	N/A	N/A	N/A	N/A
317	Stanleyville	Oviataku	0.54	2.56	1.6	2.39	2.00	N/A	N/A	N/A	N/A	N/A	N/A	N/A

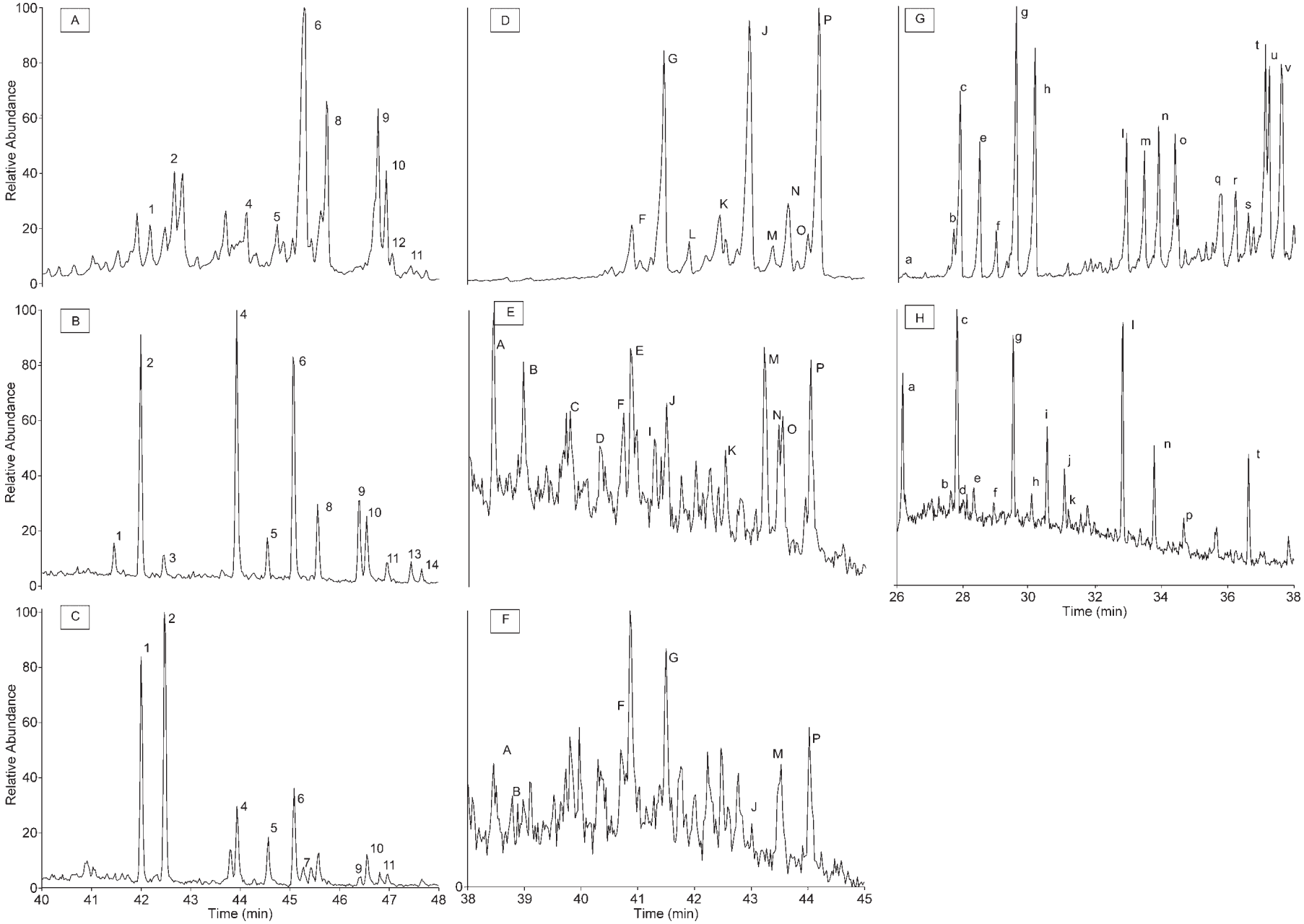

Figure 6. Hopane (A–C), sterane (D–F), and tricyclic terpane (G–H) distributions of Loia (A, D, G) and Lukuga groups (B, E, H). Panels C and F present distributions for the Lukuga coal sample (314). For peak identification, see Table 2.

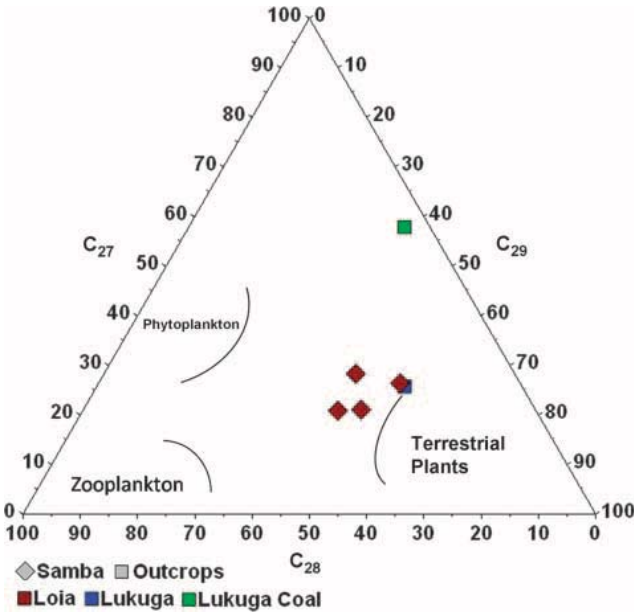

Figure 7. Relative composition of C_{27}, C_{28}, and C_{29} steranes in selected samples showing the relative abundance of C_{28} and C_{29}, indicating terrestrial plants and aquatic matter as the main source of the organic matter.

ratio, which shows a dominance of the C_{31} hopane. These ratios and the dominance of C_{29} steranes in the Lukuga samples lead to the conclusion of a mainly terrestrial OM contribution. The abundance of hopanes shows the strong contribution of bacterial OM. The sterane/hopane ratio indicates, thus, a terrigenous or microbially reworked OM for the samples of the Lukuga Group, especially the coal sample.

Samples from the Loia Group show a greater input of C_{27} steranes, most probably derived from various types of algae. The abundance of both C_{27} and C_{29} steranes leads to the assumption of a lacustrine depositional environment for the Loia Group (Figure 7). An explanation for the low diasteranes concentrations in all samples might be clay-poor sediments, that is, a carbonatic system of deposition. The low values of the C_{31}/C_{30} hopane ratio (<0.20) might indicate deposition under more lacustrine conditions, whereas higher values (>0.25) represent marine shales, carbonates, and marl source rocks. The sterane/hopane ratio gives an idea about the OM input. Steranes originate mainly from algae and higher plants, and hopanes originate from the cell material of bacteria. The highest values of the Loia Group indicate the presence of algal OM. Sterane/hopane ratios, thus, indicate higher amounts of planktonic and/or benthic algae (Moldowan et al., 1985) for the Loia samples.

Applying all of the available parameters (i.e., distribution of steranes, low diasteranes, high HI values, TS/C_{org} values), deposition in a lacustrine environment is most likely for the most prominent petroleum source rocks of the Loia Group. In general, environments with an oversaturation of carbonates occur in warm, arid climates, especially in areas where carbonate rocks are eroded in the hinterland of the lake. Comparison of the depositional environment and kind of OM of the Loia Group with other well-investigated sediments in central and east Africa revealed high similarities with sediments in Lake Tanganyika in the East African rift system. This is a mildly alkaline lake, where high sulfur and carbonate concentrations, especially high Mg and Ca concentrations, occur. The lake water displays thermal stratification that varies seasonally above an apparently permanently anoxic hypolimnion at water depths of 50 to 250 m (164 ft–820 ft) (Cohen, 1989). Because of the strongly reducing anoxic bottom waters of Lake Tanganyika, accumulation of significant quantities of autochthonous organic carbon was possible (Cohen, 1989), in addition to allochthonous OM. In Lake Tanganyika, the HI is as high as 600, with a primary productivity ranging from 400 to 500 g C/m^3 yr (Kelts, 1988). Variations in productivity are related to changes in phytoplankton and algae composition, as well as in their (periodic) abundance (Huc et al., 1990). Lake Tanganyika contains a high diversity of carbonate facies within the littoral zones of the lake, resulting from oversaturation of Ca, alkalinity of the lake waters, the presence of biogenic carbonate-producing algae, and clastic sediment accumulation on littoral platforms (Cohen and Thouin, 1987). The quality of the OM is related to the depositional environment, which is a function of the rift morphology. The delivery of clastic sediments in the system is also controlled by the basin morphology (half graben), including canyon systems, platform ramps, and structural highs.

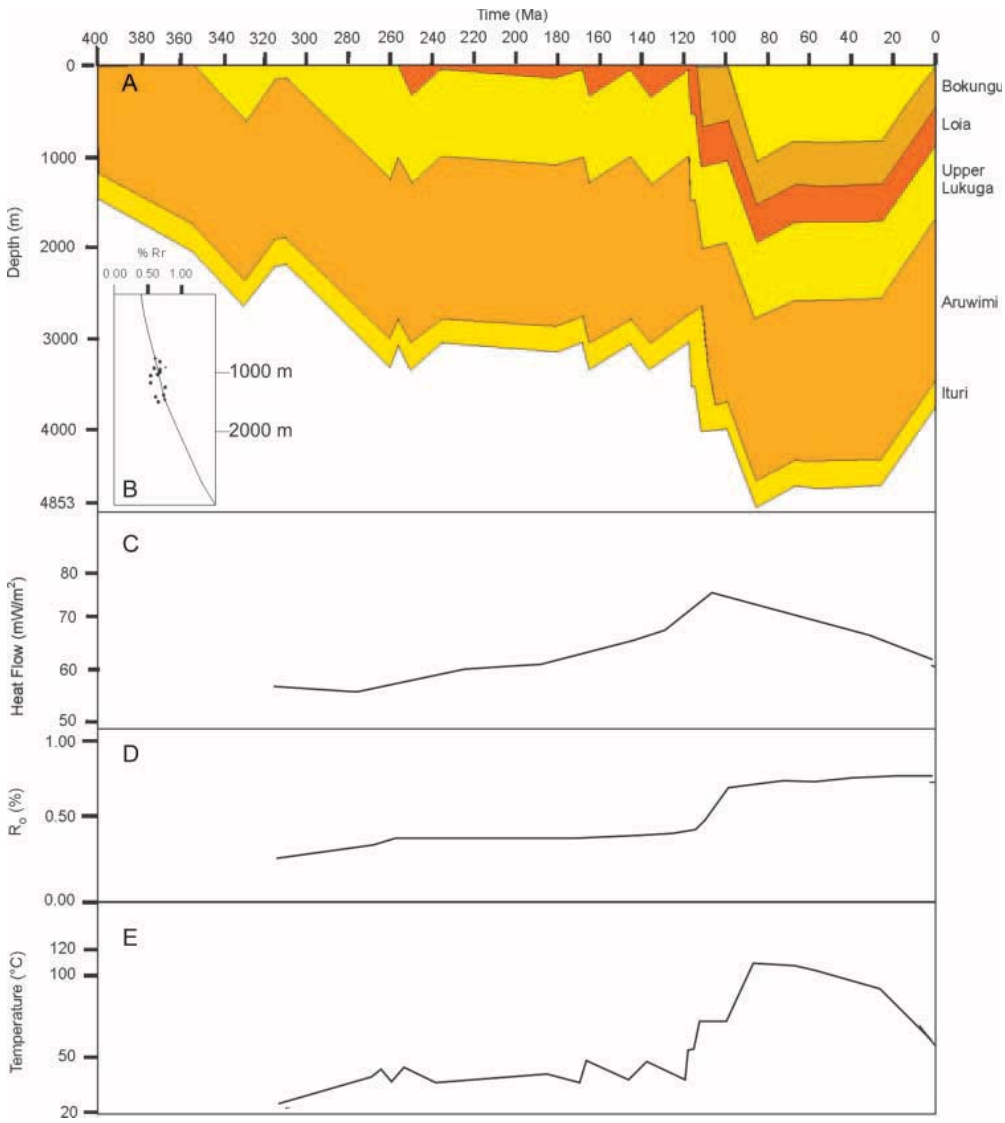

Figure 8. One-dimensional model for the Dekese well. (A) Burial history. (B) Measured (dots) and calculated (line) vitrinite reflectance (R_o, %) of Dekese well. (C) Heat-flow (mW/m^2) history. (D) Maturity history. (E) Temperature history for the Lukuga Group. Model calibration using heat flow as input and R_o as a calibration parameter.

Petroleum Potential and Maturity

The concentration of C_{org} in a rock is not sufficient for estimating the oil generation potential. Espitalié et al. (1985) and Peters (1986) recommended that source rocks with S_2 (remaining potential) more than 5 and 10 mg HC/g rock should be considered as having a good and very good source rock potential, respectively.

Outcrop samples of the Stanleyville Group are characterized by type I kerogen of excellent quality because of their high HI values (Figure 3C). Samples of the Loia Group revealed a wide variation in the HI and OI values, representing a mixture of type I and II kerogen. Both sample sets also offer R_o and T_{max} values, which are typical for maturity ranges partly within the oil window (immature–early mature). Low PI values, showing a high remaining HC generation potential, are attributed to the presence of thermally quite stable kerogen that has not yet reached temperatures high enough for significant petroleum generation. These values are supported by the n-alkane distribution patterns, which also revealed an immature to early mature stage of OM. Both Stanleyville and Loia groups can be regarded as excellent petroleum source rocks and could be part of a petroleum system, where sufficient burial and maturation occurred.

Permian–Carboniferous sediments from the Lukuga Group (Dekese well) contain much OM, but only type III to IV kerogen (Figure 3C), having a very minor gas generation potential. The T_{max}

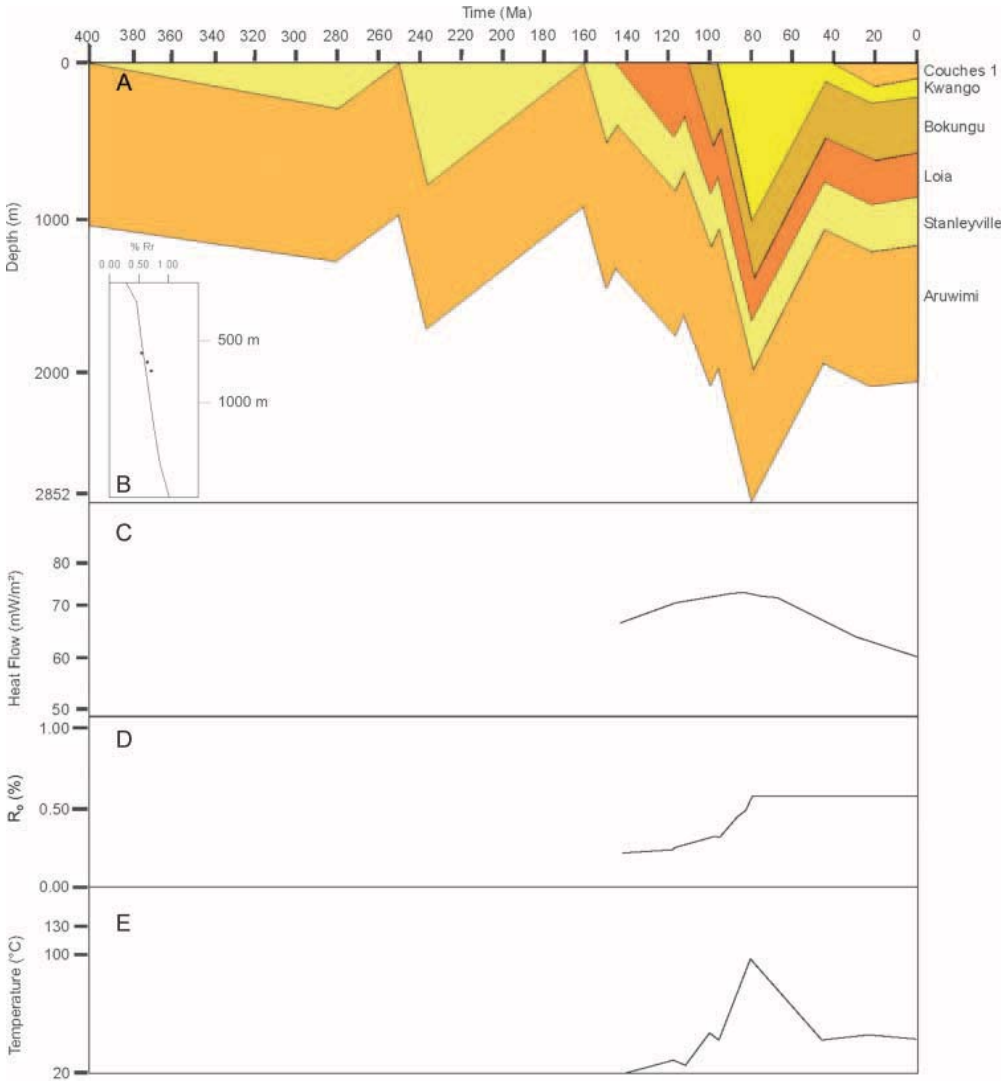

Figure 9. One-dimensional model for Samba well. (A) Burial history. (B) Measured (dots) and calculated (line) vitrinite reflectance (R_o, %) of Samba well. (C) Heat-flow (mW/m^2) history. (D) Maturity history. (E) Temperature history for Stanleyville Group. Model calibration using heat flow as input and R_o as a calibration parameter.

values indicate early mature OM, which is supported by R_o and PI values, although the latter indicates higher maturity than T_{max}. This observation is tentatively explained by the presence of abundant resedimented OM. Outcrop samples from the Lukuga Group in the Walikale area show similar results, but partly with higher maturity, as indicated by R_o data and T_{max} values. All samples contain hydrogen-poor type III kerogen with low oil generation potential. The Pr/n-C_{17} and Ph/n-C_{18} ratios confirm an early mature stage of the OM in most of these samples, and even indicate a more mature stage for the others. The coal sample from Kalemie has Pr/n-C_{17} and Ph/n-C_{18} ratios (Figure 5), which are characteristic for an early mature stage of the OM, supporting the R_o data.

The Alolo shales of the Aruwimi Group, representing type III to IV kerogen (Figure 3C), cannot be considered as a potential oil source rock with respect to their kerogen type. Nevertheless, the n-alkane distribution leads to the assumption of the presence of mature oil within these samples. Note that on the basis of C_{org} and R_o values, the Alolo shales have been generally considered as poor source rock quality. The 200-m (656-ft)-thick middle gray zone of the Alolo shales exposed along the lower course of the Aruwuimi River near Yambuya is assumed to yield as much as 1.69% C_{org}, with seven samples yielding 1% C_{org}. It was concluded in unpublished reports The Alolo shales constitute a moderate to good source rock and speculate that this unit extended over a large

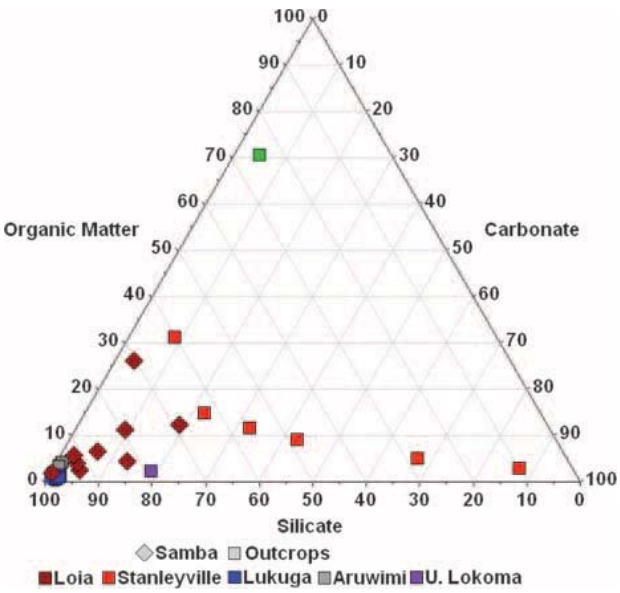

Figure 10. Original sediment compositions before sulfate reduction for some of the Congo samples.

part of the Congo Basin, predicting a large generation potential. Reanalyzing a total of 32 Alolo Shale samples from the same collection, we came to a markedly different conclusion. Our samples represent three different sections of the Alolo Shale: Malili-Banalia (10 samples) and Yambuya (18 samples) sections along the Aruwimu River and Lindi Bridge (6 samples) section along the Lindi River near Kisangani. Only the Yambuya section gave moderate C_{org} values, averaging 0.58% with a maximum of 1.83%, whereas the other sections gave average values of 0.13 (Malili-Banalia) and 0.18 (Lindi Bridge). The nine richest samples of the Yambuya section were analyzed by Rock-Eval, giving very low HI (27 on average) and relatively high OI (158 on average) (Figure 3D).

The various CPI and OEP values that were used in this study revealed values more than 1 for most samples of the Loia, Stanleyville, and Lukuga groups, indicating a low thermal maturity based on the odd preference of the n-alkanes.

The ratio of tricyclic terpanes/17α-hopanes revealed immature to early mature OM. This ratio increases with increasing thermal maturity because more tricyclic terpanes than hopanes are released from kerogen at higher levels of maturity (Aquino Neto et al., 1983). Maturity, as expressed by hopane isomerization ratios 22S/(22S + 22R), of nearly all samples shows that the OM is immature to marginally mature. The T_s/T_m ratio (18α [H]-22,29,30-trisnorneohopane [T_s]/17α[H]-22,29,30-trisnorhopane [T_m]; Table 3) is dependent on both thermal maturation and source lithology. During catagenesis, T_m is less stable than T_s; thus, the ratio of T_s to T_m should increase with maturity. In our samples, values are less than 0.53, indicating immature to marginally mature OM. The marginally mature nature of the OM is also supported by the C_{29} 17α-norhopane/C_{30} 17α-hopane ratio, where norhopane is more stable than hopane during thermal maturation.

Maturity information derived from typical sterane ratios also shows low maturity of all samples, that is, the 20S/(20S + 20R) values are all less than 0.55. The 24-ethyl-5α,14α,17α(H)-cholestane (20R) is the dominant C_{29} sterane isomer and, in general, charactistic of immature source rocks.

Burial and Temperature Histories, Uplift, and Erosion

The thermal and depositional evolution of the central part of the Congo Basin was evaluated by 1-D numerical modeling calibrated with the general geologic information and the R_o data from the Dekese and Samba wells. The modeling revealed that the deepest burial occurred during the Late Cretaceous (~80 Ma, Santonian–Campanian transition) for both wells, which is also supported by apatite fission-track results (U. Glasmacher, 2011, personal communication). In general, the calibration of a model is based on (1) heat flow and (2) deposition and erosion of the sediment packages. Because of the intracratonic nature of the Congo Basin, high heat flows can be excluded. Therefore, a high amount of deposited and eroded sequences is necessary to explain the R_o data. For the Dekese and Samba wells, erosions of, respectively, 1000 and 900 m (3280 and 2950 ft) (because 150 m [492 ft] of Late Cretaceous sediments are left in Samba well) were assumed, leading to temperatures and related maturity ranges matching with the measured R_o data. The temperature and maturation histories of both wells indicate that higher temperatures and, thus, deeper burial for the sediments of the Loia

and Lukuga groups, respectively, can be excluded; otherwise, they would show a higher R_o. Based on R_o data, it is also possible to recalculate the necessary burial depth for the sediments of the outcrop localities. The coal sample of the Lukuga coal field near Kalemie revealed an R_o of 0.47%, which implies a former burial of approximately 1500 m (~4920 ft). In the cases of the outcrop samples of the Lukuga Group in the Walikale area, a deeper burial to approximately 2500 m (~8200 ft) is necessary to reach an advanced maturity level (0.7–0.8% R_o). This mid-Cretaceous accelerated subsidence followed by Late Cretaceous uplift and erosion could be a manifestation of the Senonian basin inversion and rejuvenation that Guiraud and Bosworth (1997) evidenced for most part of Africa but is not yet reported in the Congo Basin.

The petrological investigation of the samples revealed a high amount of resedimented and allochthonous vitrinite and vitrinitelike particles in the Lukuga Group, typically with R_o values of 0.8 to 1.1%. This leads to the assumption of a provenance from older Carboniferous units containing abundant terrestrial OM. The resedimented vitrinite particles with a high reflectance (0.8–1.1%) were buried deeper (~3000–4000 m [~9840–13,120 ft]) than those with lower values and, thus, were exposed to higher temperatures (~100–130°C). These resedimented vitrinites could stem from the eastern part of the Congo Basin, where Carboniferous intervals were deposited and partly eroded. This implies a deep burial for the Carboniferous sediments in this area with later erosion. Because of the absence of terrestrial land plants before the Devonian and high abundance of terrestrial OM being typical for the Carboniferous, these sediments are preferred as source for the resedimented vitrinites in the Lukuga Group in the wells of the central Congo Basin.

CONCLUSIONS

Our data revealed two potential source rocks in the Congo Basin: sediments of the Loia and Stanleyville groups. All of the sub-Mesozoic sediments contain only a small amount of OM. Only the Lukuga Group has a higher amount of OM, which has at best a very minor gas generation potential. The high C_{org} content of the Loia and Stanleyville groups is caused by the high bioproductivity of aquatic OM (algal phytoplankton) and its preservation. Anoxic to dysoxic bottom-water conditions are interpreted for these groups because of the Pr and Ph values. Clearly, the aquatic OM of the Loia Group strongly contributed to the total OM. The amount of alginite and the HI values are high, accompanied by the presence of components in extractable HCs, which are indicative of algal OM. In addition, hydrogen-poor OM is also abundant mainly in a mixture with the algal-derived material. Especially the sediments of Lokoma and Aruwimi groups show this mixture, but also some samples of the Stanleyville Group. Clear indications of terrestrial input in these groups are the high CPI values of long-chain n-alkanes and the petrological composition.

All of the Mesozoic and Paleozoic source rocks show an early maturity, partly within the oil window (Stanleyville and Loia groups), which is indicated by T_{max} and R_o values. Based on the R_o data and the geologic setting, a former burial of 1600 m (5250 ft) for the sediments of the Loia Group is probable. The abundance of allochthonous and resedimented vitrinite in the Lukuga Group leads to the assumption of redeposition of terrestrial OM of Carboniferous sediments. Based on R_o data, the sediment outcrops of the Lukuga Group at the Walikale area, eastern margin of the Congo Basin, have been buried to a 2500-m (8200-ft) depth. The resedimented vitrinite particles in the Lukuga Group at the Dekese well even suggest burial to 3000–4000 m (9840–13,120 ft) of the now eroded Carboniferous (and Devonian) rocks at the eastern basin margin.

Because of the kind and quality of the OM of the Loia and Stanleyville groups, these sediments can be regarded as excellent potential source rocks. Considering the early mature range and the burial history of wells Dekese and Samba, we conclude that exploration for conventional oil should focus on positions in the basin where the Upper Jurassic to Lower Cretaceous sequence has reached greater maturity than in the case of the areas studied here.

REFERENCES CITED

Aquino Neto, F. R., J. M. Trendel, A. Restle, J. Connan, and P. A. Albrecht, 1983, Occurrence and formation of tricyclic and tetracyclic terpanes in sediments and petroleums, *in* M. Bjorøy et al., eds., Advaces in organic geochemistry: New York, John Wiley and Sons, p. 659–667.

Berner, R. A., 1970, Sedimentary pyrite formation: American Journal of Science, v. 268, p. 1–23, doi:10.2475/ajs.268.1.1.

Berner, R. A., 1984, Sedimentary pyrite formation: an update: Geochimica et Cosmochimica Acta, v. 48, no. 4, p. 605–615, doi:10.1016/0016-7037(84)90089-9.

Blanc, P. L., and J. Connan, 1992, Origin and occurrence of 25-norhopanes: A statistical study: Organic Geochemistry, v. 18, p. 813–828, doi:10.1016/0146-6380(92)90050-8.

Buitler, S., and B. Steiberger, 2010, Could subsidence in the Congo Basin be caused by the interplay of lithosphere deformation and mantle flow? (abs.): Conference Out of Africa: 140 years with Kevin Burke and Lew Ashwal, University of the Witwatersrand, Johannesburg, South Africa, November 15–18, 2009, Abstract volume, p. 15.

Cahen, L., 1983a, Le Groupe de Stanleyville (Jurassique supérieur et Wealdien de l'intérieur de la République du Zaïre): Révision des connaissances: Rapport des Annees 1981–1982, Royal Museum for Central Africa, Department of Geology and Mining, p. 73–91.

Cahen, L., 1983b, Brèves précisions sur l'âge des groupes crétaciques post-Weladien (Loia, Bokungu, Kwango) du Bassin intérieur du Congo (République du Zaïre): Rapport des Annees 1981–1982, Royal Museum for central Africa, Department of Geology and Mining, p. 61–72.

Cahen, L., and J. Lepersonne, 1954, État actuel des connaissances relatives aux séries mésozoïques de lìntérieur du Congo: Bulletin de la Société Belge de Géologie, v. 77, p. 20–37.

Cahen, L., J. J. Ferrand, M. J. F. Haarsma, J. Lepersonne, and T. Verbeek, 1959, Description du Sondage de Samba: Annales Musée Royal de l'Afrique Centrale (Tervuren, Belgique), série in 8°: Sciences Géologiques, v. 29, 210 p.

Cahen, L., J. J. Ferrand, M. J. F. Haarsma, J. Lepersonne, and T. Verbeek, 1960, Description du Sondage de Samba: Annales Musée Royal de l'Afrique Centrale (Tervuren, Belgique), série in 8°: Sciences Géologiques, v. 34, 115 p.

Cohen, A. S., 1989, Facies relationships and sedimentation in large rift lakes and implications for hydrocarbon exploration: examples from lakes Turkana and Tanganyika: Paleogeography, Paleoclimatology, Paleoecology, v. 70, p. 65–80, doi:10.1016/0031-0182(89)90080-1.

Cohen, A. S., and C. Thouin, 1987, Nearshore carbonate deposits in Lake Tanganyika: Geology, v. 15, p. 414–418, doi:10.1130/0091-7613(1987)15<414:NCDILT>2.0.CO;2.

Colin, J. -P., 1994, Mesozoic–Cenozoic lacustrine sediments of the Zaire Interior Basin, *in* E. Gierlowski-Kordeschand and K. Kelts, eds., Global geological record of lake basins, International Geological Correlation Programme Project 324: Cambridge, Cambridge University Press, v. 1, p. 31–36.

Crosby, A. G., S. Fishwick, and N. White, 2010, Structure and evolution of the intracratonic Congo Basin: Geochemistry, Geophysics, Geosystems, v. 11, p. 1–20, doi:10.1029/2009GC003014.

Daly, M. C., S. R. Lawrence, D. Kiun`a, and M. Binga, 1991, Late Paleozoic deformation in central Africa: A result of distant collision?: Nature, v. 350, p. 605–607, doi:10.1038/350605a0.

Daly, M. C., S. R. Lawrence, K. Diemu-Tshiband, and B. Matouana, 1992, Tectonic evolution of the Cuvette Centrale, Zaire: Journal of the Geological Society (London), v. 149, p. 539–546, doi:10.1144/gsjgs.149.4.0539.

Delvaux, D., 2001, Karoo rifting in western Tanzania: Precursor of Gondwana breakup? Contributions to geology and paleontology of Gondwana in honor of Helmut Wopfner: Cologne, Geological Institute, University of Cologne, p. 111–125.

Delvaux, D., and A. Barth, 2010, African stress pattern from formal inversion of focal mechanism data: Implications for rifting dynamics: Tectonophysics, v. 48, p. 105–128, doi:10.1016/j.tecto.2009.05.009.

Demaison, G. J., and G. T. Moore, 1980, Anoxic environments and oil source bed genesis: Organic Geochemisty, v. 2, p. 9–31, doi:10.1016/0146-6380(80)90017-0.

Dow, W. G., 1977, Kerogen studies and geological interpretations: Journal of Geochemical Exploration, v. 7, p. 77–99, doi:10.1016/0375-6742(77)90077-2.

Downey, N. J., and M. Gurnis, 2009, Instantaneous dynamics of the cratonic Congo Basin: Journal of Geophysical Research, v. B114, p. B06401, doi:10.1029/2008JB006066.

Egorov, A., and A. L. Lombard, 1962, Présence des couches de Stanleyville dans le sous-sol de Lépoldville, République du Congo (Note préliminaire): Annales de la Société Géologique de Belgique, v. 85, p. 103–109.

Espitalié, J., G. Deroo, and F. Marquis, 1985, La pyrolyse Rock-Eval et ses applications: Revue de l'Institut Français du Pétrole, v. 40, p. 563–579.

Evrard, P., 1957, Les recherches géophysiques et géologiques et les travaux de sondage dans la Cuvette Congolaise: Académie Royale des Sc. Colon., Sc. Techn. Bruxelles, v. VII, 62 p.

Evrard, P., 1960, Résultats scientifiques des missions du syndicat pour l`étude géologique et minière de la Cuvette Congolaise et travaux connexes, géodésie et géophysique: Sismique: Annales du Musee royal du Congo belge, Tervuren, 88 p.

Forte, A. M., S. Quéré, R. Moucha, N. A. Simmons, S. P. Rand, J. X. Mitrovica, and D. B. Rowley, 2010, Joint seismic-geodynamic-mineral physical modeling of African geodynamics: A reconciliation of deep-mantle convection with surface geophysical constraints: Earth Planetary Science Letters, v. 295, p. 329–341, doi:10.1016/j.epsl.2010.03.017.

Fourmarier, P., 1914, Le bassin charbonnier d'age Permo-Triassique de la Lukuga. Etude géologique de la région de la Lukuga et de la Lubumba au voisinage du lac Tanganyika: Annales du Societe geologique de Belgique, Liege, v. 41, p. C77–227.

Giresse, P., 2005, Mesozoic–Cenozoic history of the Congo Basin: Journal of African Earth Science, v. 43, p. 301–305, doi:10.1016/j.jafrearsci.2005.07.009.

Guiraud, R., and W. Bosworth, 1997, Senonian basin inversion and rejuvenation of rifting in Africa and Arabia: Synthesis and implications to plate-scale tectonics: Tectonophysics, v. 282, p. 39–82, doi:10.1016/S0040-1951(97)00212-6.

Halbich, W., F. J. Fitch, and J. A. Miller, 1983, Dating the Cape orogeny: Special Publication of the Geological Society of South Africa, Pretoria, v. 12, p. 149–164.

Harris, N. B., K. H. Freemann, R. D. Pancost, T. S. White, and G. D. Mitchell, 2004, The character and origin of lacustrine source rocks in the Lower Cretaceous synrift section, Congo Basin, west Africa: AAPG Bulletin, v. 88, no. 8, p. 1163–1184, doi:10.1306/02260403069.

Huc, A. Y., J. Le Fournier, M. Vandenbroucke, and G. Bessereau, 1990, Northern Lake Tanganyika: An example of organic sedimentation in an anoxic rift lake, *in* B. J. Katz, ed., Lacustrine basin exploration, Case studies and modern analogs: AAPG Memoir 50, p. 169–185.

Jamotte, 1931, Contribution à l'étude géologique du basin charbonnier de la Lukuga. Comité Spécial du Katanga: Annales du Service des Mines, v. 2, p. 3–44.

Kadima, E., D. Delvaux, S. N. Sebagenzi, L. Tack, and M. Kabeya, 2011a, Structure and geological history of the Congo Basin: An integrated interpretation of gravity, magnetic and reflection seismic data: Basin Research, p. 1–29, doi:10.1111/j.1365-2117.2011.00500.x.

Kadima, E., S. S. M. Ntabwoba, and F. Lucazeau, 2011b, A Proterozoic-rift origin for the structure and the evolution of the cratonic Congo Basin: Earth and Planetary Science Letters, v. 304, no. 1–2, p. 240–250, doi:10.1016/j.epsl.2011.01.037.

Katz, B. J., 1995, A survey of rift basin source rocks, *in* J. J. Lambiase, ed., Hydrocarbon habitat of rift basins: Geological Society (London) Special Publication 80, p. 213–242.

Kelts, K., 1988, Environments of deposition of lacustrine petroleum source rocks, *in* A. J. Fleet, K. Kelts, and M. R. Talbot, eds., Lacustrine petroleum source rocks: Geological Society (London) Special Publication, v. 40, p. 3–26.

Kontorovich, A. E., A. N. Izosimova, A. A. Kontorovich, E. M. Khabarov, and I. D. Timoshina, 1996, Geological structure and conditions of the formation of the giant Yurubchen-Tokhomo zone of oil and gas accumulation in the Upper Proterozoic of the Siberian Platform: Russian Geology and Geophysics, v. 37, p. 156–185.

Lallier-Vergès, E., P. Bertrand, A. Y. Huc, D. Bückel, and P. Tremblay, 1993, Control of the preservation of organic matter by productivity and sulfate reduction in marine anoxic sediments: Kimmeridgian shales from Dorset (United Kingdom): Marine and Petroleum Geology, v. 10, no. 6, p. 600–605.

Lawrence, S., and M. M. Makazu, 1988, Zaire's Central basin: Prospectivity outlook: Oil & Gas Journal, v. 86, p. 105–108.

Lepersonne, J., 1951, Les subdivisions du système du Karroo au Kwango (Congo belge): Annales de la Société Géologique de Belgique, v. 74, p. B123–139.

Lepersonne, J., 1977, Structure geologique du basin intérieur du Zaire: Bulletin du Académie Royale de Belgique, classe des Sciences 5, Bruxelles, p. 941–965.

Le Roux, J. P., 1995, Heartbeat of a mountain: Diagnosing the age of depositional events in the Karoo (Gondwana) basin from the pulse of the Cape orogen: Geologische Rundschau, v. 84, p. 626–635, doi:10.1007/s005310050029.

Linol, B., M. De Wit, F. Guillochau, A. Boven, and E. Barton, 2011, Sedimentology and chronostratigraphy of two deep boreholes in the Congo Basin (abs.): 23rd Colloquium on African Geology, Johannesburg, South Africa, January 8–14, 2011, Abstract volume, p. 243.

Littke, R., 1993, Deposition, diagenesis and weathering of organic matter-rich sediments: Lecture notes in earth sciences: Berlin, Springer-Verlag, 216 p.

Littke, R., D. R. Baker, and J. Rullkötter, 1991a, Keys to the depositional history of the Posidonia Shale (Toarcian) in the Hils syncline, northern Germany, *in* R. V. Pearson and T. H. Tyson, eds., Modern and ancient shelf anoxia: Geological Society (London), v. 58, p. 311–334.

Littke, R., U. Bayer, G. Gajewski, and S. Nelskamp, eds., 2008, Dynamics of complex intracontinental basins: The central European basin system: XXIV, 414 p. Berlin, Springer.

Littke, R., U. Klussmann, B. Krooss, and D. Leythaeuser, 1991b, Quantification of calcite-, pyrite-, and organic matter-loss due to weathering of Toarcian black shales and effects on kerogen and bitumen characteristics: Geochimica et Cosmochimica Acta, v. 55, p. 3369–3378, doi:10.1016/0016-7037(91)90494-P.

Lombard, A. L., 1960, L'extension méridionale des couches de Stanleyville, Congo belge (Note préliminaire): Bulletin of the Geological Society of Belgium, v. 69, p. 23–27.

Lückge, A., M. Boussafir, E. Lallier-Vergés, and R. Littke, 1996, Comparative study of organic matter preservation in immature sediments along the continental margins of Peru and Oman: Part I. Results of petrographical and bulk geochemical data: Organic Geochemistry, v. 24, no. 4, p. 437–451, doi:10.1016/0146-6380(96)00045-9.

Moldowan, J. M., P. Sundararaman, and M. Schoell, 1985, Sensitivity of biomarker properties of depositional environment and/or source input in the lower Toarcian of southwest Germany: Organic Geochemistry, v. 10, no. 4–6, p. 915–926, doi:10.1016/S0146-6380(86)80029-8.

Newton, A. R., R. W. Shone, and P. W. Booth, 2006, The Cape fold belt, *in* M. R. Johnson, C. R. Anhaeusser, and R. J. Thomas, eds., The geology of South Africa: Pretoria, Geological Society of South Africa, Johannesburg and Council for Geoscience, p. 521–530.

Passau, G., 1923, La géologie du bassin des schistes bitumineux de Stanleyville (Congo belge): Annales du Societe des Geologists Belgique, Publications related to belgian Congo, v. 19, no. 1921-1922, p. 91–243.

Pedersen, T. F., and S. E. Calvert, 1990, Anoxia versus productivity: What controls the formation of organic carbon-rich sediments and sedimentary rocks: AAPG Bulletin, v. 74, p. 454–466.

Peters, K. E., 1986, Guidelines for evaluating petroleum source rocks using programmed pyrolysis: AAPG Bulletin, v. 70, p. 318–329.

Peters, K. E., and K. M. Moldowan, 1991, Effect of source, thermal maturity and biodegradation on the distribution and isomerization of homohopanes in petroleum: Organic

Geochemistry, v. 17, p. 47–61, doi:10.1016/0146-6380(91)90039-M.
Petmecky, S., L. Meier, H. Reiser, and R. Littke, 1999, High thermal maturity in the lower Saxony Basin: Intrusion or deep burial?: Tectonophysics, v. 304, p. 317–344, doi:10.1016/S0040-1951(99)00030-X.
Philippi, G. T., 1965, On the depth, time and mechanism of petroleum generation: Geochimica et Cosmochimica Acta, v. 29, no. 9, p. 1021–1049, doi:10.1016/0016-7037(65)90101-8.
Schull, T. J., 1988, Rift basins of interior Sudan: Petroleum exploration and discovery: AAPG Bulletin, v. 72, p. 1128–1142.
Sebagenzi, M. N., G. Vasseur, and P. Louis, 1993, First heat flow density determinations from southeastern Zaire (central Africa): Journal of African Earth Sciences, v. 16, no. 4, p. 413–423, doi:10.1016/0899-5362(93)90100-5.
Senglaub, Y., R. Littke, and M. R. Brix, 2006, Numerical modeling of burial and temperature history as an approach for an alternative interpretation of the Bramsche anomaly, lower Saxony Basin: International Journal of Earth Sciences, v. 95, p. 204–224, doi:10.1007/s00531-005-0033-y.
Shanmungam, G., 1985, Significance of coniferous rain forests and related organic matter in generating commercial quantities of oil, Gippsland Basin, Australia: AAPG Bulletin, v. 69, p. 1241–1254.
Sinninghe Damsté, J. S., and J. Köster, 1998, An euxinic southern North Atlantic Ocean during the Cenomanian/Turonian oceanic anoxic event: Earth Planetary Science Letters, v. 158, p. 165–173, doi:10.1016/S0012-821X(98)00052-1.
Stein, R., and R. Littke, 1990, Organic-carbon-rich sediments and paleoenvironment: Results from Baffin Bay (ODP-Leg 105) and the upwelling area off northwest Africa (ODP-Leg 108), *in* A. Y. Huc, ed., Deposition of organic facies: AAPG Studies in Geology 30, p. 41–56.
Surkov, V. S., M. P. Grishin, A. I. Larichev, V. I. Lotyshev, N. V. Melnikov, A. Eh. Kontorovich, A. A. Trofimuk, and A. N. Zolotov, 1991, The Riphean sedimentary basins of eastern Siberia province and their petroleum potential: Precambrian Research, v. 54, p. 37–44, doi:10.1016/0301-9268(91)90067-K.
Sweeney, J. J., and A. K. Burnham, 1990, Evaluation of a simple model of vitrinite reflectance based on chemical kinetics: AAPG Bulletin, v. 74, p. 1559–1570.
Tankard, A., H. Welsink, P. Aukes, R. Newton, and E. Settler, 2009, Tectonic evolution of the Cape and Karoo basins of South Africa: Marine Petroleum Geology, v. 26, p. 1379–1412, doi:10.1016/j.marpetgeo.2009.01.022.
Taylor, G. H., M. Teichmüller, A. Davis, C. F. K. Diessel, R. Littke, and P. Robert, 1998, Organic petrology: Berlin, Borntraeger, 704 p.
Thurow, J., H. J. Brumsack, R. Littke, P. Meyers, and J. Rullkötter, 1992, The Cenomanian/Turonian boundary event in the Indian Ocean: A key to understand the global picture: Geophysical Monograph, v. 70, p. 253–273.
Tissot, B., and D. H. Welte, 1984, Petroleum formation and occurrence: New York, Springer-Verlag, 699 p.
Tyson, R. V., 2001, Sedimentation rate, dilution, preservation, and total organic carbon: Some results of a modeling study: Organic Geochemistry, v. 32, p. 333–339, doi:10.1016/S0146-6380(00)00161-3.
Tyson, R. V., and T. H. Pearson, 1991, Modern and ancient continental shelf anoxia: Geological Society (London) Special Publication, v. 58, 470 p.
Veatch, A. C., 1935, Evolution of the Congo Basin: Memoirs of the Geological Society of America 3, 184 p.
Verbeek, T., 1970, Géologie et lithologie du Lindien (Précambrien Supérieur du nord de la République Démocratique du Congo): Annales Musée Royal de l'Afrique Centrale (Tervuren, Belgique), série in 8°, v. 66, 311 p.
Wang, P. R., 1993, Mass chromatogram atlas of biomarkers (in Chinese): Bejing, Petroleum Industry Press, p. 20–21.
Waples, D. W., H. Kamata, and M. Suizu, 1992, The art of maturity modeling: Part 1. Finding a satisfactory geological model: AAPG Bulletin, v. 76, p. 31–46.
Welte, D. H., and M. N. Yalcin, 1987, Basin modeling: A new comprehensive method in petroleum geology: Organic Geochemistry, v. 13, p. 141–151, doi:10.1016/0146-6380(88)90034-4.
Wygrala, B. P., 1988, Integrated computer-aided basin modeling applied to analysis of hydrocarbon generation history in a northern Italian oil field, *in* L. Matavelli and L. Novelli, eds., Advances in organic geochemistry: Organic Geochemistry, v. 13, p. 187–197, doi:10.1016/0146-6380(88)90039-3.